Interaction of disturbance agents on Norway spruce : A mechanistic model of bark beetle dynamics integrated in simulation framework WINDROT

Honkaniemi, Juha

2018-11-24

Honkaniemi , J , Ojansuu , R , Kasanen , R & Heliövaara , K 2018 , ' Interaction of disturbance agents on Norway spruce : A mechanistic model of bark beetle dynamics integrated in simulation framework WINDROT ' , Ecological Modelling , vol. 388 , pp. 45-60 . https://doi.org/10.1016/j

http://hdl.handle.net/10138/319641
https://doi.org/10.1016/j.ecolmodel.2018.09.014

Interaction of disturbance agents on Norway spruce: a mechanistic model of bark beetle dynamics integrated in simulation framework WINDROT

Juha HONKANIEMI[1,2], Risto OJANSUU[1], Risto KASANEN[3], Kari HELIÖVAARA[3]

[1] Natural Resources Institute Finland (Luke), Management and Production of Renewable Resources, Latokartanonkaari 9, FI-00790 Helsinki, Finland (juha.honkaniemi@luke.fi, risto.ojansuu@luke.fi)

[2] Institute for Silviculture, University of Natural Resources and Life Sciences Vienna, Peter-Jordan Strasse 82, 1190 Vienna, Austria (juha.honkaniemi@boku.ac.at)

[3] University of Helsinki, Department of Forest Sciences, Faculty of Agriculture and Forestry, Latokartanonkaari 7, 00014 University of Helsinki, Finland (risto.kasanen@helsinki.fi, kari.heliovaara@helsinki.fi)

For correspondence:
Juha Honkaniemi

Current address:
Insitute for Silviculture, University of Natural Resources and Life Sciences Vienna
Peter-Jordan Strasse 82, 1190 Vienna, Austria
juha.honkaniemi@boku.ac.at Declarations of interest: none

Abstract

Interaction of disturbance agents may cause cascading effects in forests. The three most important disturbance agents of Norway spruce (*Picea abies*) in northern Europe are *Heterobasidion* root rot, wind and the European spruce bark beetle (*Ips typographus*). In this study, we present a mechanistic individual agent based model to simulate the dynamics of the bark beetle and integrate it in the simulation framework WINDROT to further study the interactive dynamics of root rot, wind and bark beetles. We carried out model performance analysis concluding that the model is sensitive to the parameters of optimal bark thickness for reproduction. Stand level interaction between wind and bark beetle disturbances was also evaluated against field data. The stand level simulations show the interaction between the disturbance agents; the root rot increases wind disturbance and bark beetles benefit from wind fallen trees. No direct interaction was found in the simulation study between the root rot and bark beetles. Further experimental research and large scale simulation studies are needed to better understand the underlying mechanisms in the interaction between the disturbance agents.

Keywords: bark beetle, *Ips*, disturbance interaction, *Picea abies*, wind disturbance, root rot

1 Introduction

Bark beetles are well-known to cause significant disturbances all over the globe in the coniferous forests (Raffa et al., 2015). Recently, the most serious large-scale outbreaks have occurred in western North America by the mountain pine beetle (*Dendroctonus ponderosae* Hopkins) (Safranyik and Wilson, 2006). In Europe, *Ips typographus* (L.), Coleoptera, Curculionidae, Scolytinae is causing significant damages in Central and northern Europe (Seidl et al., 2011). Many bark beetle species attack trees in high numbers to overcome tree resistance, which is dependent on the tree vigor (Mulock and Christiansen, 1986; Raffa and Berryman, 1983). Hence, when the bark beetle population is low, weakened trees with low resistance are required for breeding and when population increases, the beetles can attack healthy, living trees.

Norway spruce (*Picea abies* (L.) Karst.) is economically one of the most important tree species in northern Europe. The managed Norway spruce stands currently face three major disturbance agents; root and butt rot caused by *Heterobasidion* species complex, wind storms and European spruce bark beetle (*Ips typographus*). All of these agents cause significant economic losses, and their impact is predicted to increase under the projected climate change (Müller et al., 2014; Peltola et al., 2010; Seidl et al., 2014).

Interaction in the disturbance dynamics may lead to cascading effects when disturbances increase the subsequent disturbances caused by another agent (Buma, 2015). On Norway spruce dominated forests in northern Europe, the most well-known regime of compounding disturbances is the one including root rot, wind and bark beetles: wood decay decreases the tree stability against wind (Giordano et al., 2012), bark beetles benefit from weakened, wind-

fallen trees (Bouget and Duelli, 2004; Komonen et al., 2011) and the root and butt rot is spreading rapidly in dead trees, roots and stumps (Bendz-Hellgren et al., 1999). One of the best examples of the cascading effects is the winter storm Gudrun in 2005 in the Götaland province in Sweden, where approximately 75 Mm^3 of trees were fallen (Anonymous, 2006). The stands with root decay were the most vulnerable for wind disturbance (Oliva et al., 2008). The operations to salvage the wind-thrown trees took time, which facilitated bark beetle mass attack in the landscape causing also serious disturbance in the subsequent years (Långström et al., 2009).

Even though the dynamics of the major disturbance agents affecting Norway spruce have been described with mechanistic models over the years (e.g. Fahse and Heurich, 2011; Gardiner et al., 2000; Honkaniemi et al., 2014; Peltola et al., 1999; Pukkala et al., 2005; Seidl et al., 2007), there are very few models including the interactive dynamics between these disturbance agents. Several bark beetle models include interaction with wind disturbance (e.g. Louis et al., 2016b; Potterf and Bone, 2017) and Western Root Disease Model (WRDM; Frankel, 1998), developed for similar system in North America, incorporates multiple agents in the simulations. However, the WRDM lacks the underlying interactivity between disturbance agents as the interactions are user-specified input values.

Honkaniemi et al. (2017a) presented a simulation framework WINDROT to simulate the interaction between root and butt rot caused by *Heterobasidion* species complex and wind disturbances. In this study, we present a mechanistic agent based model for *Ips typographus* integrated into the WINDROT framework. The biology of bark beetles and the factors affecting the outbreaks are rather well known (Seidl et al., 2016; Wermelinger, 2004) and there are already several mechanistic models to simulate the bark beetle dynamics (Fahse and

Heurich, 2011; Kautz et al., 2014, 2013; Louis et al., 2016b; Potterf and Bone, 2017; Seidl et al., 2007). Even though many of the models include the interaction between wind disturbance and subsequent bark beetle dynamics, they lack other agents or the underlying mechanisms and dynamic interactions. Our aim was to include dynamic interaction in the simulations by combining mechanistic models for three different disturbance agents.

Root rot on Norway spruce is most often caused by *Heterobasidion* species in the Nordics. They cause great economic losses throughout the Northern Hemisphere (Woodward et al., 1998) by reducing the timber value as well as causing growth losses and mortality. In addition, they decrease the supportive strength of the trees against wind storms (Giordano et al., 2012). *Heterobasidion* species spread by two mechanisms; spores infect fresh wood surfaces and subsequent mycelia grows through root contacts from tree to tree (Garbelotto and Gonthier, 2013; Piri and Valkonen, 2013; Piri, 2003). Forest management and especially fresh stumps have created an optimal spreading route for the disease. The spore deposition has high spatio-temporal variation and in the Nordics the highest infection probabilities occur during the summer months (Brandtberg et al., 1996; Möykkynen and Kontiokari, 2001; Witzell et al., 2011). In case of Norway spruce, root rot advances from root system up into the stem mainly decaying the heartwood (Stenlid and Redfern, 1998). However, it can challenge the tree vigor by entering into functional sapwood and therefore causing growth losses (Bendz-Hellgren and Stenlid, 1997; Oliva et al., 2012, 2010).

Wind causes mechanical loading on the canopy and stem which lead to tree failure if the tree resistive strength is exceeded. The overall bending moment is a sum of the horizontal forces created by the wind and the vertical forces created by the gravity (Peltola, 2006). The mechanical support of the root system resists these forces against uprooting and stem

120 resistance moment against stem breakage (Peltola, 2006). The trees break or uproot if the
121 wind load exceeds the tree mechanical strength. Because several variables affecting this
122 strength, such as tree species, height-diameter ratio and rooting depth, are subject to forest
123 management (Ancelin et al., 2004; Peltola et al., 1999), it plays a significant role in the
124 control of wind disturbances.
125
126 European spruce bark beetle males pioneer the attacks and produce the aggregation and anti-
127 aggregation pheromones released during the attack on the trees (Bakke et al., 1977) to
128 overcome the tree resistance threshold. Trees suitable for bark beetle attack need to have bark
129 that is thick enough to offer protection and nutrition for the bark beetles during their life
130 stages under the bark. This limits the trees to have at least a 2.5 mm thick bark (Grünwald,
131 1986). If a suitable tree is found and the tree resistance is overcome, bark beetles can use the
132 tree for reproduction. Due to preference for the weakened trees as reproduction material when
133 the population is low, bark beetle outbreaks are often subsequent to wind disturbances
134 providing massive amounts of timber in the forest (Bouget and Duelli, 2004; Eriksson et al.,
135 2005; Komonen et al., 2011).
136
137 The objective of this paper is to describe an individual agent based model for European
138 spruce bark beetle and include that in a simulation framework WINDROT (Honkaniemi et
139 al., 2017a) to study the potential interactions between the three disturbance agents; root rot,
140 wind and bark beetles. We present the model in detail as well as test the submodel sensitivity
141 and evaluate parts of the model against field data following the principles of pattern-oriented
142 modelling (POM) (Grimm and Railsback, 2012). To our knowledge, this study is the first
143 simulation work considering these three disturbance agents and their interactive dynamics. In

addition, we have carried out simulations to analyze the model performance and sensitivity in tree and stand scale.

2 Materials and methods

2.1 Model description

The new mechanistic model BBDYN, described in this article, is developed to simulate the bark beetle dynamics within an existing simulation framework WINDROT (Honkaniemi et al., 2017a). The model is based on the basic structure presented in SAMBIA model (Fahse and Heurich, 2011) with several modifications and parametrizations. The novelty of BBDYN lies in the development of key mechanisms of bark beetle dynamics (reproduction, aggregation and tree colonization) to be tree-size dependent as the underlying interaction mechanisms between different disturbance agents could be only related to tree growth and the disturbance effects on tree growth. We present submodels where the reproduction is related to the colonizable bark area of each tree based on the optimal bark thickness for *Ips typographus*. The aggregation caused by pheromones and the overcome of tree resistance are based on the tree growth.

The basic structure of the BBDYN model was based on the SAMBIA model (Fahse and Heurich, 2011) with several modifications. The key differences between the models are: i) change from grid-based spatial layout (SAMBIA) to random coordinates of trees (BBDYN); ii) addition of absent host dynamics (SAMBIA) to complex stand dynamics affected by forest management simulated with MOTTI stand level decision support system (Hynynen et al., 2014; Salminen et al., 2005) (BBDYN); and iii) replacement of static, non-size-dependent

parameters (SAMBIA) with tree-size-dependent parameters with bark thickness model (BBDYN). The preference of weakened trees for bark beetle reproduction was included in SAMBIA, but the weakened trees were randomly selected from the landscape rather than including the interactive dynamics.

BBDYN model was included in the simulation framework WINDROT (Honkaniemi et al., 2017a) including already three previously published models (i.e. MOTTI, Hmodel and HWIND, see Appendix 1 for more description of these models). In this framework MOTTI stand level decision support system (Hynynen et al., 2014; Salminen et al., 2005) simulates the tree growth and stand dynamics affected by different forest management options. Hmodel (Honkaniemi et al., 2017b, 2014) simulates the *Heterobasidion* species complex dynamics in space and time in stand scale and decreases the tree anchorage as well as causes growth losses and tree mortality. HWIND (Peltola et al., 1999) simulates the wind disturbance by calculating critical wind speeds for each tree of the stand, which are further compared to the annual maximum wind speed on the location of the stand. WINDROT framework simulations are by default run on a rectangular area of 1 ha (100 x 100 m) with a buffer zone of 8 m on each side of the area (see Appendix 1). The stand environment is assumed uniform with similar forest continuing beyond the simulation area borders.

The model description follows the ODD (Overview, Design concepts, Details) protocol for describing individual- and agent-based models (Grimm et al., 2010, 2006). The abbreviations used in this paper are presented in Table 1 with explanations as well as with parameter values if applicable.

2.2 Purpose

The purpose of the model is to simulate the *Ips typographus* dynamics in Norway spruce stands. In addition, the model integrates the economically most important disturbance agents of Norway spruce into the stand dynamics and simulates the potential interactions and compounding effects between these disturbance agents, in the WINDROT simulation framework.

2.3

BBDYN model includes beetles as entities interacting with three other agents (trees, *Heterobasidion* and wind) included in the other models of the WINDROT framework. Each bark beetle individual is described with state variables of flying ability (groups of "strong", "average" and "weak" bark beetles) and gender (only flight of males is simulated). Reaction to aggregation and anti-aggregation is dependent on the individual's flying ability. Species-specific optimal bark thickness (minimum and maximum bark thicknesses for reproduction) defines which trees are suitable for bark beetle colonization and reproduction. The population is formed of individuals with different flying abilities forming groups of beetles which are further divided into two flying cohorts each. This way all the beetles do not disperse at the same time.

Trees are described with state variables of diameter at 1.3 m height (*dbh*) and height (*h*). MOTTI describes the stand as a group of sample trees represented by the state variables and each sample tree representing a certain number of trees. Hmodel then creates a spatial stand based on these sample trees (see full details in (Honkaniemi et al., 2017b, 2014). Hmodel adds information on trees whether they are infected or not, the extent of decay in root system

and stem and whether the tree suffers growth losses due to root rot. HWIND predicts critical wind speeds for each tree and comparison of those against local wind data provides information whether trees can tolerate the wind effect or not (uprooted/broken). Bark beetle individuals attack trees and if they exceed the tree's resistance threshold, colonize the tree for further reproduction. Unsuccessful attacks (ie. number of attacking beetles less than tree resistance threshold) result in the death of the beetles and the tree remains uninfested.

2.4 Process overview and scheduling

The default time step of BBDYN model is one year. During this time step, the order of models in WINDROT framework is following; stand dynamics and tree growth in MOTTI, fungal dynamics in Hmodel and wind disturbance dynamics in HWIND. After wind disturbance dynamics, the bark beetle dynamics are simulated through the following processes in the following order; (i) dispersal, (ii) colonization, (iii) reproduction, and (iv) mortality (Fig. 1). Within the dispersal process the individual beetles disperse according to their flying ability ("strong", "average", "weak"). These groups are further divided into flying cohorts flying in consecutive waves, in order to be exposed to pheromones. Calculated values are assigned to beetles after each cohort simulation. Beyond the dispersal, beetles are considered as one population and values are assigned after calculating them for the whole population. This principal of scheduling applies also to other models with trees, fungi and wind.

2.5 Design concepts

2.5.1 Emergence

Interactions between wind and bark beetles or root rot and bark beetles are not fixed in the model and are expected to emerge from simulations. Interactions depend on the growth of the trees. In addition, the number of attacking bark beetles per tree is not fixed to any limit, but is regulated by the reactance of individuals to aggregation and anti-aggregation pheromones. There is one major built-in feature in the model affecting the behavior of individuals. The initial beetle population is assumed to be only on the stand edge, whereas later generations disperse within the stand in more random pattern.

2.5.2 Adaptation

Beetles adapt to the population levels in trees by emitting aggregation and anti-aggregation pheromones during the dispersal and thus trying to avoid overpopulation of trees which affects the reproduction success. Re-emergence of beetles is not included.

2.5.3 Objectives

Each beetle generation is grouped into three groups by their expected flying ability (“strong”, “average” and “weak”). These groups of individuals are formed with an objective to avoid overpopulation in trees by affecting their i) dispersal range and ii) reactance to pheromones.

2.5.4 Sensing

Bark beetles sense during the dispersal stage only the pheromones emitted by other beetles attacking a tree. They do not sense tree state variables such as if a tree is uprooted or otherwise weakened. However, the weakening of a tree (death, growth losses by root rot) reduces the tree resistance against beetles and thus when that limit is met earlier compared to intact trees, the beetles start emitting their anti-aggregation pheromones earlier in weakened trees.

269

270 2.5.5 Interaction

271 The interactions between different disturbance agents and bark beetles are indirect and
272 mediated through the tree growth.

273

274 2.5.6 Stochasticity

275 Stochasticity is included in the WINDROT simulation framework in forming the spatial stand
276 structure (ie. locations of trees and stumps, stump diameters not provided by MOTTI). In
277 addition all probabilistic parameters included stochasticity. In the BBDYN model the
278 dispersal of beetles was random along with probabilistic parameters included in other
279 submodels.

280

281 2.5.7 Collectives

282 Individuals belong to three groups by their expected flying ability ("strong", "average" and
283 "weak"). These groups are further divided into cohorts whom then fly one after another.

284

285 2.5.8 Observation

286 Tree level output includes information of the number of beetles attacking the tree, success of
287 the attack, the number of beetles reproducing and the number of offspring. Other tree level
288 output includes tree state variables and tree level data regarding other disturbance agents (e.g.
289 decay dimensions within stem, critical wind speeds). In stand level output the number of trees
290 killed by bark beetles is collected along with number of trees affected by other disturbance
291 agents (see Honkaniemi et al., 2017a, 2014).

292

293

294 2.6 Initialization

295 The simulation for stand and *Heterobasidion* dynamics start from regeneration after clear-cut
296 of the previous tree generation. In WINDROT framework, Hmodel is responsible for creating
297 the spatial structure of the stand within 100m*100m square with 8m buffer (see Honkaniemi
298 et al., 2017b, 2014). Tree and stump locations are random with minimum between-tree
299 distances determined by the user. This creates stochasticity in the initialization of the
300 WINDROT framework. The BBDYN model described in this paper is initialized after stand
301 exposure for wind disturbance at the time t_W after the clear-cut of a neighboring stand on one
302 side of the simulation area including the buffer zone on that side (Honkaniemi et al., 2017a).
303 An initial bark beetle population (pop_{BB}) for that time is given by the user. The clear-cut
304 creates a stand edge adjacent to the simulated stand, which has a warming effect favoring
305 bark beetle reproduction (Peltonen, 1999). This effect in the model is included however only
306 through the first dispersal of initial bark beetle population (pop_{BB}) at the stand edge. After the
307 initialization of BBDYN the framework proceeds at default on simulation steps of one year
308 for a period of 10 years.
309
310 2.7 Input data
311 The user-defined input variable of the BBDYN model is the initial number of bark beetles in
312 the simulation area at t_W (pop_{BB}). We assume that the initial sex ratio of pop_{BB} is 1:1. In
313 BBDYN, only the movement of males is simulated and only males are considered to
314 contribute to the initial attacks and aggregation to overcome the tree resistance. Hence, the
315 initial pop_{BB} is divided by two. Otherwise, the model does not use any data outside from the
316 data that is within the WINDROT framework.
317
318 2.8 Submodels

319

320 (i) Dispersal

321

322 Bark beetles are distributed in two ways into the trees within the stand depending on the
323 simulation step. At t_W, the first simulation step for bark beetle dynamics, the males of the
324 initial bark beetle population ($0.5*pop_{BB}$) are distributed randomly along the stand edge. In
325 the consecutive simulation steps, dispersal of bark beetles from reproduction trees is
326 simulated as described by Fahse and Heurich (2011) using Gaussian Kernel Random Walk
327 (Eq. 1), where the probability for the bark beetle to fly from its origin (0, 0) to location (x, y)
328 is modeled as a function of landing coordinates (x, y), diffusion coefficient D and time for
329 dispersal t_D. As time step by default is one year, t_D=1, each bark beetle is given a single
330 random coordinate to fly to.

331

332 (1) $P(x, y, D, t) \sim \exp(-\frac{x^2+y^2}{4Dt_D})$

333

334 We divided the bark beetle generation into three groups by their expected flying ability
335 ("strong", "average" and "weak"), in a similar way that was done in SAMBIA model (Fahse
336 and Heurich, 2011). Each of these groups are further divided into two flight cohorts forming
337 a total of six flight cohorts, as all the bark beetles do not fly at the same time in the nature.
338 Cohorts were flying in order from strongest to weakest (i.e. strong1, strong2, average1,
339 average2, weak1, weak2). The diffusion coefficient D was transformed to correspond meters
340 used in our simulation framework compared to the grid approach by Fahse and Heurich
341 (2011) (Table 1). The values for each of the groups flight ability were 644, 286 and 72 m^2
342 $season^{-1}$ for "strong", "average" and "weak", respectively.

343

After the first dispersal, the bark beetles are redistributed to suitable host trees (living or one year time from death at maximum) (e.g. Eriksson et al., 2005; Louis et al., 2016a, 2014) based on possible i) aggregation or ii) anti-aggregation pheromones from trees in the vicinity. If such trees do not exist, the bark beetle is moved to a nearest suitable tree ($A_{bark} > 0$). If trees are not in the vicinity (< 13.5 m), the bark beetle is considered to die due to loss of energy. The surroundings of the simulated hectare is assumed to continue similar behind the borders (except the upwind gap) and thus, if the random coordinates of a bark beetle exceed the simulation area, another bark beetle from the surroundings would replace it with a random coordinate within the simulation area.

The limit values for the production of aggregation and anti-aggregation pheromones were assumed to be related to a tree-specific threshold of resistance (D_{def}, see section 2.2.2 "Colonization and mortality of trees"). We assumed that aggregation pheromones are produced by the first bark beetles entering the tree and pheromone production changes from aggregation to anti-aggregation when the tree resistance threshold is achieved (Birgersson, 1989). The first two cohorts of "strong" bark beetles do not react to pheromones (Nêmec et al., 1993). However, bark beetles from "average" and "weak" flying cohorts react to the aggregation as they are assumed to have lower body weight and therefore to react more strongly to aggregation (Nêmec et al., 1993). In addition, only beetles of the group "strong" are affected by the anti-aggregation pheromones (Schlyter et al., 1989). Individuals from the same flight cohort were not affected by pheromones produced by the same flight cohort (i.e. one flight cohort was assumed to fly at the same time and disperse unrelated to each other). The effective radii of a catchment area around a tree where pheromones are produced were 13.5 and 4.5 m for aggregation (r_{agg}) and anti-aggregation (r_{antagg}), respectively (Fahse and Heurich, 2011).

(ii) Colonization and mortality of trees

Successful attack of bark beetles occurs when the number of bark beetles attacking the tree overcomes the threshold of the tree resistance (Mulock and Christiansen, 1986; Raffa and Berryman, 1983). This threshold is related to the tree vigor index (*tvig*) which is the relative area of annual growth of sapwood area (*tvig=BAi/SA*). The threshold value for tree defense (N_{def}) is thus tree-specific variable depending on the tree growth (i_{dbh}) and tree diameter (*dbh*) (Eq. 2) based on the study by Mulock and Christiansen (1986). Trees where N_{def} is overcome by the attacking beetles are categorized first "infested" and after reproduction "dead".

(2) $N_{def} = 90 \cdot \exp(0.24 \cdot tvig)$

(iii) Reproduction

Reproduction occurs in successfully colonized "infested" trees. Reproduction rate and the number of offspring (D_{f1}, Eq. 3) are based on the density of female bark beetles (D_{fem}) per 100 cm^2 colonizable bark area obtained from Anderbrant et al. (1985) including the intra-specific larval mortality. We assumed that on average every male, which has successfully infested a tree, reproduces with two females (Annila, 1971). To produce the overall number of offspring from one tree (N_{f1}), the density of offspring produced in 100 cm^2 (D_{f1}) is further multiplied with the colonizable bark area (A_{bark}) (Eq. 4) and assumed to have sex-ratio of 1:1 for next simulation step population.

(3) $D_{f1} = D_{fem} \cdot 38.8 \cdot e^{-0.87 \cdot D_{fem}^{0.45}}$

394 (4) $N_{f1} = Df1 \cdot A_{bark}$

395

396 To predict the colonizable bark area for reproduction in each tree of the stand (A_{bark}), the bark
397 thickness in tree *j* (B_{lj}) at different tree heights (*l*) was modeled based on the data by Vuokila
398 and Väliaho (1980) including 1024 Norway spruce from 128 sample plots in Finland. Data
399 included bark thicknesses from 9 relative tree height (x=0.01, 0.02, 0.06, 0.10, 0.20, 0.30,
400 0.50, 0.70, 0.85).

401

402 A linear mixed model (*nls* from *nlme* package) (R Development Core Team, 2015) was fitted
403 for the bark thickness (B_{lj}) as a function of section height within tree (*l*). The polynomial
404 formulation was based on the Fibonacci series used for stem curve model by Laasasenaho
405 (1982) (Eq. 5). Model parameters, the standard deviation of the random effect of tree *j* (u_j),
406 and the standard deviation of the random measurement effect (ε_{lj}) are presented in Table 2.

407

408 (5) $B_{lj} = a_1 x_j + a_2 (dbh \cdot x)_j + a_3 x_j^2 + a_4 x_j^3 + a_5 x_j^5 + a_6 x_j^8 + a_7 x_j^{13} + u_j + \varepsilon_{lj}$

409

410 (6) $x = 1 - \frac{l}{h}$

411

412 The main fixed independent variables were relative point of the height (*x,* Eq. 6) and diameter
413 at breast height (*dbh*). The first degree depends on the *dbh*, where tree was the grouping
414 variable *j*. Autocorrelation within the data (φ, Table 2) (measurements within single tree are
415 not independent) was taken into account by first order continuous autocorrelation function
416 (*corCAR1*).

417

Further, the height within tree for minimum (B_{min}=2.5 mm (Grünwald, 1986)) and maximum bark thickness (B_{max}=*no limit* (Grünwald, 1986)) for bark beetle reproduction, l_{Bmin} and l_{Bmax}, were calculated, respectively. The total colonizable bark area was finally calculated as a sum of 10 equal length trapezoid parts of the colonizable bark area (Eq. 7):

(7) $$A_{bark} = \sum_{i=0}^{9} \frac{(p_{(lmax+i\cdot(0.1\cdot h_{Abark}))} + p_{(lmax+(i+1)\cdot(0.1\cdot h_{Abark}))})}{2} (0.1 h_{Abark}) \cdot 100$$

Here p is the perimeter at height l, l_i, and l_{i+1} are the heights of the begin and end of the i:th part and 0.1*h_{Abark} is tenth of the height of the colonizable bark area (0.1*h_{Abark}=*0.1*(lmin-lmax)**h). The perimeters at each relative height were predicted according to the stem taper curve by Laasasenaho (1982). Finally, the area was transformed to 100 cm^2 to correspond the reproduction rate equation.

(iv) Mortality of bark beetles

Mortality of bark beetles occurs in BBDYN in three different ways; i) intra-specific competition at the larval phase, ii) predation by antagonists and iii) winter mortality. The intra-specific competition is included in the reproduction rate by Anderbrandt et al (1985) in section “Reproduction”.

For the predation effect of antagonists, we used the full submodel for antagonists from SAMBIA (see Fahse and Heurich 2011, section 2.2.5 part 4d and Appendix A for mathematical description), where the submodel for antagonist effects consists of two parts; i) probability for the antagonists to find a colonized tree used for bark beetle reproduction, and ii) survival probability of the larvae under predation. Fahse and Heurich (2011) studied the submodel in detail and presented sensitivity analysis for the submodel parameters. We chose

443 to use constant values for the sigmoid curve parameters of the probability for antagonists to
444 find an infested tree. These upper and lower limit parameter values were $p_{find}(1)$=0.999 and
445 $p_{find}(0)$=0.03, respectively. If the antagonists would find the colonized tree, then the constant
446 survival probability for the larvae under predation was 0.05. According to Fahse and Heurich
447 (2011), by using this survival probability the risk for outbreak is medium (~0.5).
448
449 The winter mortality after each simulation step affected the population at the end of the
450 growth season. Winter mortality was parametrized to be 0.4 for this simulation study
451 (Austarå and Midtgaard, 1986; Faccoli, 2002; Poolak, 1975).
452
453 2.5 Outline of simulations
454
455 The new submodel of BBDYN, colonizable bark area model within the reproduction process,
456 was evaluated in two parts. First, tree level simulations were carried out to analyze the
457 sensitivity of the reproduction to changes in colonizable bark area (A_{bark}). Colonizable bark
458 area was calculated for three individual trees of different diameters at breast height (*dbh*=20,
459 30 and 40 cm) and tree height (*h*=20, 25 and 30 m) with combinations of different minimum
460 and maximum bark thicknesses (b_{min}=[2.0, 2.5, 3.0 mm] and b_{max}=[4.0, 5.0, *no limit* mm]).
461 Second, the colonizable bark areas from stand level simulations (see below) were evaluated
462 against field data including measured bark areas in attacked trees of various sizes (Weslien
463 and Regnander, 1990) (Table 3).
464
465 The simulated stand was set up to represent a typical Norway spruce stand growing on a
466 *Myrtillus* site type (Cajander, 1949) in southern Finland on mineral soil with temperature sum
467 (*tsum,* sum of degrees by which the daily average temperature exceeds +5 °C) of 1300 d.d.

468 The site was prepared before planting trees with density of 1800 ha^{-1}, and seedling survival
469 was 90 %. Forest management followed the current management recommendation for Finnish
470 forestry (Äijälä et al., 2014). The rotation length was fixed to 61 years in all scenarios, and
471 the second thinning was set to take place at the age of 44 years at the same time with the final
472 cut of the neighboring stand. This exposed the stand to wind disturbance. The timing of the
473 first commercial thinning depended on the stand basal area and varied between simulated
474 replications and scenarios. This also created variable stand densities and dimensions prior to
475 the second thinning. The default simulation step in the simulations (beyond the wind/bark
476 beetle period) was 5 years, but it adjusts to the timing of forest management operations. The
477 effect of root rot by *Heterobasidion* was simulated using three different root rot risk scenarios
478 used earlier also by Honkaniemi et al. (2017a); low-, medium- and high-risk scenarios (Table
479 4). These scenarios address both infections mechanisms of the fungi; primary spread via
480 basidiospores and secondary spread through root contacts. The previous stand was clear-cut
481 in the summer-time during active spore production season and all thinnings were winter-time
482 operations with zero spore loads. No control measures were taken to prevent *Heterobasidion*
483 infections.
484
485 The wind disturbances were simulated for a 10-year period in simulation steps of one year
486 after the second thinning as described by Honkaniemi et al. (2016). Long-term statistics for
487 the annual probability of the maximum 10-min average wind speed at 10 meters high above
488 ground for Helsinki-Vantaa Airport (Peltola et al., 2010) were used. Maximum winds were
489 assumed to occur when there was no frost in the ground. Subsequent bark beetle dynamics
490 were then simulated in three scenarios (low BB, med BB and high BB) for the initial bark
491 beetle population (pop_{BB}) at the time of the wind exposure (t_W=44): 1) 10 000, 2) 25 000 and

3) 40 000 beetles ha^{-1}, respectively. Therefore, altogether 9 different scenarios (3 root rot scenarios * 3 bark beetle scenarios) were simulated in stand scale.

All the disturbance models are mechanistic models with stochastic features such as tree location within the simulated area and wind speed. Therefore, the simulation error should be stabilized. The number of replicated simulations required in the model in stand scale was studied by running the model with various amounts of replications (2–400). Previously, the inclusion of HWIND in the simulation framework increased the required number of replications to 200 (Honkaniemi et al., 2017a). In this study, the simulation error for the number of trees killed by bark beetles was considered sufficiently small (<0.5 tree/ha) with 200 replications in all risk scenarios over the 10-year simulation period and within one year with largest variation in the output. Therefore, 200 replications were used in the subsequent simulations. Annual and 10-year simulation period averages were calculated based on the output of these 200 replications.

We compared the model predictions against field data including wind and bark beetle disturbances (Eriksson et al., 2007, 2005) (Table 3). This data was collected from Southern Finland including 60 windthrow areas (some omitted due to various reasons, see Eriksson et al. 2005, 2007) and corresponds quite well to our simulated stand conditions and environmental conditions for bark beetle dynamics. It includes data of number of wind damaged trees, dead standing trees prior to the wind event (proxy for bark beetle presence), size of the windthrow area, share of attacked windthrown trees, number of trees killed by bark beetles in the adjacent 4 years after the major wind disturbance event as well as the total number of egg galleries in the windthrown trees in those areas in the year after wind disturbance. These were compared against simulation output from WINDROT framework.

517 Unfortunately, the field data did not include records on root rot nor population levels for the
518 initial bark beetle population.
519
520 # 3 Results
521
522 ## 3.1 Model evaluation
523
524 ### 3.1.1 Tree level sensitivity analysis
525
526 The tree level sensitivity analysis showed that the reproduction of bark beetles (number of
527 offspring from one tree, N_{fl}) in all the three trees was sensitive to the changes in the
528 maximum bark thickness (b_{max}), but not for the minimum bark thickness (b_{min}) (Fig. 2). The
529 effect of maximum bark thickness in N_{fl} increased with increasing tree size. By default there
530 was no limit for the maximum bark thickness for bark beetle reproduction. Reducing the b_{max}
531 to 4.0 mm decreased the reproduction in 40 cm tree 72 870 beetles from the scenario where
532 b_{max} was not limited (Fig. 2). The reduction in 30 cm tree was 45 670 beetles and in 20 cm
533 tree 23 280 beetles. The reduction of the minimum bark thickness b_{min} from parameter value
534 2.5 mm to 2.0 mm increased the number of offspring from the tree at maximum 330 beetles,
535 and increase of the b_{min} from 2.5 to 3.0 mm decreased the reproduction at maximum by 480
536 beetles. Respectively, the changes in 30 cm tree were 450 and 630 and in 40 cm tree 580 and
537 770 beetles. The maximum number of offspring per tree with the default parameter values
538 b_{min}=2.5 and b_{max}=*no limit* mm were 26 370, 48 550 and 76 000 from trees with *dbh* 20, 30
539 and 40 cm, respectively.
540
541 ### 3.1.2 Colonizable bark area on stand level

The colonizable bark areas for bark beetle reproduction (A_{bark}) of infested trees from all scenarios were compared against the results by Weslien and Regnander (1990) (Fig. 3). The simulation output shows that the model's colonizable bark areas with b_{min} of 2.5 mm for bark beetle suitability was in line with the field data (Weslien and Regnander, 1990). Similar patterns are reported in other field studies as well where *I. typographus* beetles occupied almost the whole stems with decrease in density of egg galleries in the last 20% of the relative height (Schlyter and Anderbrant, 1993). The maternal gallery density per BB scenario (average over *Heterobasidion* scenarios) was 755, 895, and 842 m^{-2} for low, medium and high BB risk scenarios, respectively.

3.1.3 Stand level output against field data

Stand level output was compared against field data by (Eriksson et al., 2007, 2005). The total number of egg galleries in the wind damaged trees of first year after exposure was in many replicates overestimated compared to the field data in low and medium BB scenarios (Fig. 4A and 4D). The share of bark beetle attacked wind damaged trees out of all wind attacked trees was overestimated slightly by the model in both scenarios (Fig. 4B and 4E). The number of first year wind damaged trees was compared against the number of trees killed by bark beetles in the consecutive four years (Fig. 4C and 4F). The low risk scenario was in line with the field observations with no previous bark beetle damages (Fig. 4C). Both the model output and field data show low levels of spruce mortality. However, the medium BB risk scenario overestimated the spruce mortality when compared against the field data with recent spruce mortality prior to the study period suggesting a higher initial population (Fig. 4F).

567 3.2 Stand level results

568

569 Comparison of all the disturbances together at the stand level showed that the root rot risk
570 level increased both the overall number of infections in the stand and the number of
571 infections where decay had reached the stem (Fig. 5). In all nine scenarios the number of root
572 rot infected trees was significantly higher than the number of wind or bark beetle disturbed
573 trees. In high root rot risk scenario, the overall number of infections reached an asymptote
574 where almost all of the trees in the stand had an infection in some part of their root system.

575

576 The stand level results of the nine different scenarios indicate that mortality due to bark
577 beetles occurred only in few simulated replications when the initial bark beetle population
578 *popBB* was low (initially 10 000 beetles ha^{-1}) indicating that the initial population *popBB* was
579 too low to cause any damages (Fig. 6). Therefore, the bark beetle disturbances are not visible
580 at all in Fig. 5 which includes average values over the 200 iterations. Increase in the initial
581 bark beetle population significantly increased the number of trees dying due to bark beetle
582 attack. In both medium and high BB risk scenario (initially 25 000 beetles ha^{-1} and 40 000
583 beetles ha^{-1}, respectively) the number of trees killed by the bark beetles continued throughout
584 the simulated 10 year period. The annual maximum number of dead trees due to bark beetles
585 was below 1 tree ha^{-1} in low BB scenario and below 14 and 40 trees ha^{-1} in medium and high
586 BB scenarios, respectively. The mean annual mortality rate over the 10 year simulation
587 period was 0.07, 8.97 and 19.04 trees ha^{-1} in the low, med and high BB scenarios (over the
588 *Heterobasidion* scenarios), respectively.

589

590 The wind damages increased with the increasing root rot risk (Fig. 7). Majority of the wind
591 damages occurred during the first year after the stand was exposed for wind in all scenarios

592 (year 45). This was seen also in the number of wind damaged trees colonized and used for
593 bark beetle reproduction during the first years of the simulation period (Fig. 8). However,
594 trees were damaged by wind throughout the simulation period and those trees were used by
595 bark beetles for reproduction. The number of infested wind damaged trees was below 21 trees
596 per year in low BB risk scenario and the bark beetle population decreased over time with
597 most of the replicates having bark beetle population only on the initial year. The overall share
598 of colonized wind damaged trees out of all bark beetle infested trees over the 10-year
599 simulation period was close to 50 % in all nine scenarios (Fig. 6 and 8). However, in both
600 medium and high BB risk scenarios, the effect of increasing wind damages with increasing
601 root rot incidence actually started to decrease the bark beetle effect as there were less trees to
602 attack and kill for such a large population of bark beetles.
603
604 We also compared the tree vigor index (*tvig)* of healthy trees and trees with root rot infection
605 but found no significant difference and therefore no significant differences in the resistance
606 threshold against bark beetles. This was due to the only small decreases in the relative growth
607 due to decay in sapwood in the simulated scenarios. The lowest relative annual growth levels
608 were 0.96, 0.98 and 0.93 in low, medium and high risk scenarios. In addition we didn't find
609 any significant effect of bark beetle caused mortality on subsequent root rot infection rates.
610
611 The number of attacking males per tree in the successfully infested trees varied from 56 to 11
612 560 beetles in all of the simulated scenarios. The average numbers of attacks per tree were
613 significantly lower in wind damaged trees compared to standing trees. Average number of
614 males attacking wind damaged trees was 140, 370 and 510 in the low, medium and high BB
615 risk scenarios, respectively. The corresponding numbers for healthy trees were 700, 1350 and
616 1400 males per tree. However, the wind damaged trees were also smaller and slender in

617 dimensions and therefore had smaller colonizable bark areas, partly explaining the difference
618 (Fig. A2). Other factors explaining the difference were lower threshold for producing anti-
619 aggregation and the fact that most the trees were wind damaged earlier in the rotation thus
620 leaving them smaller than the healthy trees attacked later during the outbreak.
621
622 4 Discussion
623
624 The main objective in the development of the BBDYN model described in this study was to
625 simulate interactions between different disturbance agents in Norway spruce stands with the
626 WINDROT framework. The key findings from the model performance analysis were that
627 bark beetle induced mortality of trees occurred only quite infrequently when the initial bark
628 beetle population was low (< 10 000 bark beetles ha^{-1}). Mortality due to bark beetles over 10-
629 year simulation period occurred in medium and high bark beetle risk scenarios. Root rot
630 increased the wind disturbances, which further played a significant role in the bark beetle
631 dynamics as the increasing amount of wind damaged trees increased the number of wind
632 damaged trees colonized by bark beetles. However, the wind damages also reduced the
633 number of living trees and thus decreased the number of living trees colonized by bark
634 beetles especially in the high root rot risk scenario (Fig. 6 & 7).
635
636 The key feature of the BBDYN model is the bark beetle dynamics to be tree-size dependent.
637 To our knowledge there are no models incorporating the colonizable bark area for bark beetle
638 reproduction, although many parameter values, such as attacks, number of egg galleries or
639 reproduction rate, are commonly measured from the field as a number per bark area. The bark
640 offers protection and food during the life stages under the bark. Therefore, the bark has to be
641 thick enough to cover an adult bark beetle and provide food during the larval stage. The

642 inclusion of colonizable bark area and tree vigor index enables the BBDYN to use such field
643 results and further enhance the parametrization of the model in the future. It also creates the
644 possibility to better simulate the interspecific interactions between different bark beetle
645 species. Bark beetles share similar dynamics of reproduction, but different species are often
646 segregated within a tree to different parts of the stem (Grünwald, 1986).
647
648 The tree level results showed that the simulated reproduction is sensitive to the changes of the
649 maximum colonizable bark thickness for bark beetle reproduction (Fig. 2). The maximum
650 bark thickness was significant for all trees, whereas minimum bark thickness was not
651 significant for any trees. The colonizable bark area was evaluated against results by Weslien
652 and Regnander (1990). They measured the colonized bark area in pheromone-baited and non-
653 baited trees with different tree height. The colonizable bark areas from stand scale simulation
654 results were well in line with the field data by Weslien and Regnander (1990) (Fig. 3).
655 Weslien and Regnander (1990) had egg galleries from stem base to tree top without any
656 significant vertical gradient, whereas our modelling limited out the tree tops with thinnest
657 bark. The suggestion of minimum bark thickness by Grünwald (1986) is based on the body
658 size of the adults and interspecific competition with other smaller bark beetle species, such as
659 *Pityogenes chalcographus* L. Schlyter and Anderbrant (1993) showed that the gallery density
660 of *I. typographus* started to decrease in the last third of the stem and significantly decreased
661 for the final sixth of the stem. Meanwhile, the gallery density of a competing species *I.*
662 *duplicatus* (Sahlb.) increased in the top part. Recent study by Grodzki and Gąsienica Fronek
663 (2017) studying infestation rates and reproduction success under several bark thicknesses
664 reported very minor effects on both variables. However, the study was conducted only until
665 2mm bark thickness and do not therefore offer information whether colonization and
666 reproduction is successful under bark thickness of less than 2mm. These field results and our

667 sensitivity analysis indicate that even though there is uncertainty on the minimum bark
668 thickness for the *I. typographus* reproduction, the effect of tree tops for the overall
669 reproduction success are small as the bark area contribution is relatively small.
670
671 Validation and evaluation of complex models such as the one presented in this manuscript is
672 difficult due to the number of variables and complexity of the system. In the previous
673 manuscripts describing other models of the WINDROT framework (Honkaniemi et al.,
674 2017a, 2017b, 2014), the models have been partially evaluated, meaning that parts of the
675 model output have been evaluated against available field data. We have tried to follow the
676 steps of pattern-oriented modelling (POM) (Grimm and Railsback, 2012) and "evaludation"
677 (Augusiak et al., 2014) while developing this simulation framework. The structure of the
678 individual models as well as the whole framework was evaluated with several iterations and
679 the quality of data was assessed while developing the submodels. In addition, we evaluated
680 some parameters and submodels by following the POM principles (see Table 3).
681
682 Comparison of the whole model against field data has been impossible as such data does not
683 exist in large enough extent mainly for two reasons. First, varying forest stand conditions, the
684 stochastic nature of disturbances and the time span for root rot damages (over tree
685 generations) would require a massive amount of field data to cover all of these various
686 conditions and it would also need to span preferably over decades to catch the slow spread of
687 root rot fungi. In this study, we compared the simulation output against interaction data for
688 wind and bark beetles (Eriksson et al., 2007, 2005) to detect if the model can produce
689 patterns observed in the field data. The data is limited to low initial population levels (no
690 record of real population levels in the field data, but recently dead standing trees were used as
691 a proxy for this), but the comparison of the number of egg galleries, share of attacked wind

692 damaged trees, and spruce mortality by bark beetles suggests that the simulation results are
693 the same order of magnitude when our low BB scenario was compared against stands with no
694 recent dead trees (Fig. 4A-C) and medium BB scenario against stands where Eriksson et al.
695 (2007) detected recently dead trees (Fig. 4D-F). The number of egg galleries after the wind
696 event were slightly higher in our model compared to the field data (Fig. 4A and D)
697 suggesting that it either overestimates the number of egg galleries or that the initial
698 population numbers were higher in our simulations. In both scenarios, the wind damaged
699 trees were colonized as in the field data. However, the field data was lacking many sites with
700 large wind disturbance (Fig. 4B and E). In addition, we calculated all attacked trees whether
701 they were successfully colonized or not. If only successfully colonized trees were calculated,
702 the values were little bit lower, but still in line with the field data (data not shown). Spruce
703 mortality was well in line with the field data in low BB risk scenario (Fig. 4C), but
704 overestimated in medium BB risk scenario (Fig. 4F). This could be an issue of discrepancies
705 in the initial conditions or interpretation of the field data. Recently, the bark beetle
706 monitoring in Finland has shown that the populations vary roughly between the low and
707 medium BB risk scenarios' initial populations (Neuvonen et al., 2017, 2016). In addition, it is
708 important to remember that we used only one scenario for the antagonists whereas Fahse and
709 Heurich (2011) show that the model can be sensitive to the parameters of that submodel. All
710 in all, we consider that the model was able to produce similar patterns observed in the field
711 data. However, we have noted the limits of the field data and further data is needed to cover a
712 more broad range of initial states and interaction scenarios (i.e. different bark beetle
713 populations and intensities of wind damage.
714
715 Stand level results showed that there were interaction effects between root and wind
716 disturbance intensity as well as with the subsequent bark beetle damages, although the wind

717 damaged trees were not preferred by any assumptions within the model during the dispersal
718 of the beetles. The beetles only benefitted from the weakened trees through the lowered
719 resistance threshold. In our study the root rot incidence increased the wind disturbance
720 intensity and aided the bark beetle population as well as the beetles were able to reproduce in
721 the wind damaged trees. However, the increasing wind damages also decreased the mortality
722 of standing trees by bark beetles. The interaction may be counterintuitive compared to the
723 common idea on the interaction between wind disturbance and bark beetles (e.g. Komonen et
724 al., 2011). However, this effect is most likely due to the small size of our simulation area. The
725 wind damages decreased the number of trees in the stand especially in the high root rot risk
726 scenario and less living trees were left in the stand to be attacked by bark beetles. A negative
727 correlation was seen especially in the medium and high BB risk scenario with the increasing
728 root rot and wind disturbance incidence (Fig. 6 & 7). Simulations over larger area or
729 landscape level could show better the interaction between wind damages and subsequent bark
730 beetle damages. In larger scale, the bark beetle population would have also more space to
731 disperse. Landscape level analysis would also reveal patterns of stand replacing disturbances
732 (e.g. expansion of disturbed areas in time), which could be further used for model evaluation
733 by comparing the model results against remote sensing data. In all scenarios, wind damaged
734 trees increased the bark beetle population and the intensity of wind damages prolonged the
735 bark beetle population suppression (Fig. 6 & 7). Eriksson et al. (2007, 2005) showed that the
736 number of wind damaged trees increased the mortality due to bark beetles. They also found
737 that the diameter of the wind damaged trees was the most significant variable explaining the
738 mortality. Therefore, it is crucial to run large scale simulations with BBDYN and WINDROT
739 framework in the future to study and analyze the effect of timing of the exposure of the stand
740 to winds and thus the effect of stand mean diameter on wind damages and subsequent bark
741 beetle induced mortality.

742

743 Direct interaction effect between the root rot and bark beetle damages (i.e. root decay
744 weakening the tree significantly and lowering the tree resistance threshold against bark beetle
745 attack) was not significant in our simulations. The growth reduction due to the root rot was
746 low in all scenarios and therefore there were only minor changes in the tree resistance
747 threshold against bark beetles. However, the intensity of decay rate clearly increases the stand
748 vulnerability to wind damages (Honkaniemi et al., 2017a; Oliva et al., 2008; Whitney et al.,
749 2002) and therefore increases the risk for subsequent bark beetle attacks. We didn't notice
750 any significant effect on the root rot infection rates after wind and bark beetle disturbances
751 (Fig. 5) where the dead trees infected by the root rot would have speeded up the disease
752 dynamics (threefold increase in the fungal spread rate in the root system of dead trees and
753 stumps compared to living trees). It is most likely that the effects are not visible over short
754 time span and would need either longer rotation length or simulation of an adjacent tree
755 generation.

756

757 When the effect of all three disturbances are compared together in terms of affected stem
758 numbers (Fig. 5), it is clear that the root rot affects far more trees than even wind and bark
759 beetle disturbed trees combined. However, it is important to keep in mind that the root rot
760 causes mortality on Norway spruce only in few cases whereas all wind and bark beetle
761 disturbed trees are dying affecting the stand dynamics more dramatically. The effect of the
762 pathogen infections are seen over a long period and would accumulate over tree generations.

763

764 Weslien et al. (1989) found that a limit value for bark beetle induced tree mortality would be
765 around 15 000 beetles per baiting trap group corresponding loosely to our initial bark beetle
766 population values. In their study, traps were placed 300m from each other and therefore

767 "catchment" area for a trap group would have been roughly 7.1 ha (radius of 150 m).
768 Assuming that capture rate of traps would be 10% (Wermelinger, 2004) of the whole
769 population within this area, the population per hectare with 15 000 beetle catch would have
770 been 8 800 beetles. In the stand level simulations, there were only few dead trees when the
771 initial bark beetle population was low (pop_{BB}=10 000) and even the increasing wind damage
772 intensity did not increase the mortality rate of trees by bark beetles. However, in medium and
773 high bark beetle risk scenarios (pop_{BB}=25 000 and 40 000, respectively) the bark beetle
774 related mortality was higher and mortality rates increased suggesting that the simulation
775 study results were in line with the field data (Weslien et al., 1989). In addition, the number of
776 attacking males per tree as well as the number of offspring produced per tree was well in line
777 with field studies (Eriksson et al., 2005; Gonzalez et al., 1996; Louis et al., 2014).
778
779 The dispersal submodel was adopted from SAMBIA with parametrization. In addition, due to
780 the rather small simulation area in WINDROT framework for bark beetle dynamics (one
781 hectare with 8 m buffer zone), the dispersal flight pattern and distance were not considered to
782 affect results significantly. During the dispersal in the model, 95 % of the groups "strong",
783 "average" and "weak" are distributed over areas of 2.5, 1.1 and 0.3 ha, respectively. Due to
784 this and the assumption that a random coordinates within the simulation area are assigned for
785 every single bark beetle leaving the area (i.e. mimicking the spread from the surrounding
786 areas), the dispersal in BBDYN can be considered almost random. Franklin and Grégoire
787 (1999) reported that only 1 % of the emerging beetles disperse within one hectare area around
788 the reproduction tree in a pheromone-free environment. It is significantly less than the
789 dispersal areas in BBDYN, where almost all of the dispersing beetles stay within few
790 hectares. However, we didn't consider this an issue due to the small simulation area. In case

WINDROT is used in landscape level, the bark beetle dispersal should be considered in more detail.

Redistribution of the bark beetles is regulated with the production of aggregation and anti-aggregation pheromones. That occurs in much smaller scale than the initial flight dispersal and was thus given more weight in the development of BBDYN. We also modified the response of different flight cohorts to pheromones from SAMBIA. In BBDYN "strong" bark beetles are not considered to respond to aggregation at all although the very first of them start to produce them. Only "average" and "weak" flight cohorts with lower body weight and fat content respond to the aggregation pheromones. On the other hand, only "strong" beetles respond to the repelling anti-aggregation pheromones. The aggregation pheromones are produced until the tree resistance threshold is achieved and from there on the pheromone production changes to anti-aggregation. However, due to the different responses to the pheromones, the threshold may be exceeded greatly and the overpopulation of the tree may lead to a reduced reproduction rate. For colonized trees the overpopulation happened in our simulations for each tree, but only in few cases in that extent that it would have affected the reproduction significantly. It is important to note that tree resistance threshold and density for overpopulation do not go hand in hand. Tree resistance threshold may be low especially in weakened trees, but the optimal reproduction is usually reached with higher densities.

There are two major points of concern in the BBDYN model. First, we don't take into account sister broods, re-emerging of the adults due to the density of attacks or the effects of the density of the offspring to future reproduction, flight abilities or pheromone production (Anderbrant et al., 1985). We considered the effect of these minor to the dynamics in the model, but the inclusion of them should be considered especially in the landscape level

simulations as all of them affect the dispersal and further the reproduction. Second limitation is the lack of phenology in the model which has an effect on the bark beetle development and on the number of bark beetle generations per year. Climate data and the bark beetle phenology were excluded from the BBDYN during the development as the temporal resolution of the WINDROT framework is in minimum one year and dynamics within one year are not simulated in detail. In addition, other models of the framework do not take into account climate data yet. However, it is essential in the future to include climate response into all models incorporated in the framework. Stand microclimate should perhaps also be taken into account as it would direct the bark beetle dispersal within stand from random to favor more the stand edges (Peltonen, 1999).

5 Conclusions

The BBDYN mechanistic model incorporated in the WINDROT simulation framework provides novel approach to assess the interactions of three most significant disturbance agents of Norway spruce and to analyze the effects of the risks posed by these disturbances to the forest management. The flexible structure of the model and especially the use of the new bark area model enables the BBDYN to be used for other bark beetle species in the future with parameterization. Model was able to produce similar patterns as the limited field data available for model evaluation. Although *Ips typographus* is one of best studied bark beetle species, the study revealed that further experimental research is still needed. Especially data is needed related to the potential interactions between weakened trees and bark beetles during the dispersal stage. Also the tree resistance and the underlying mechanisms of interactions between disturbance agents need to be studied more profoundly in the future together with field data and simulation modeling.

841 Acknowledgements:

842

843 This study was carried out at the University of Helsinki, Natural Resources Institute of
844 Finland and University of Natural Resources and Life Sciences Vienna. The study was
845 financially supported by The Foundation for Research of Natural Resources in Finland (Grant
846 No. 2015090). We thank for the two anonymous reviewers for their most invaluable
847 comments improving the quality of the manuscript.

848

849 References:

850

851 Ancelin, P., Courbaud, B., Fourcaud, T., 2004. Development of an individual tree-based
852 mechanical model to predict wind damage within forest stands. For. Ecol. Manage. 203,
853 101–121.
854 Anderbrant, O., Schlyter, F., Birgersson, G., 1985. Intraspecific competition affecting parents
855 and offspring in the bark beetle Ips typographus. Oikos 45, 89–98. doi:10.2307/3565226
856 Annila, E., 1971. Sex ratio in Ips typographus L. (Col. scolytidae). Ann. Entomol. Fenn. 37,
857 7–14.
858 Anonymous, 2006. Stormen 2005 – en skoglig analys. [in Swedish] (No. 1), Meddelande.
859 Augusiak, J., Van den Brink, P.J., Grimm, V., 2014. Merging validation and evaluation of
860 ecological models to "evaludation": A review of terminology and a practical approach.
861 Ecol. Modell. 280, 117–128. doi:10.1016/J.ECOLMODEL.2013.11.009
862 Austaå, Ø., Midtgaard, F., 1986. On the longevity of Ips typographus L. adults. Zeitschrift
863 für Angevandte Entomol. 102, 106–111.
864 Bakke, A., Froeyen, P., Skatteboel, L., 1977. Field response to a new pheromonal compound
865 isolated from Ips typographus. Naturwissenschaften 64, 98–99.
866 doi:10.1007/BF00437364
867 Bendz-Hellgren, M., Brandtberg, P.-O., Johansson, M., Swedjemark, G., Stenlid, J., 1999.
868 Growth Rate of Heterobasidion annosum in Picea abies Established on Forest Land and
869 Arable Land. Scand. J. For. Res. 14, 402–407. doi:10.1080/02827589950154104
870 Bendz-Hellgren, M., Stenlid, J., 1997. Decreased volume growth of Picea abies in response to
871 Heterobasidion annosum infection. Can. J. For. Res. 27, 1519–1524. doi:10.1139/x97-
872 104
873 Birgersson, G., 1989. Host tree resistance influencing pheromone production in Ips

874 typographus (Coleoptera: Scolytidae). Ecography (Cop.). 12, 451–456.
875 doi:10.1111/j.1600-0587.1989.tb00922.x
876 Bouget, C., Duelli, P., 2004. The effects of windthrow on forest insect communities: a
877 literature review. Biol. Conserv. 118, 281–299. doi:10.1016/j.biocon.2003.09.009
878 Brandtberg, P.O., Johansson, M., Seeger, P., 1996. Effects of season and urea treatment on
879 infection of stumps of Picea abies by Heterobasidion annosum in stands on former
880 arable land. Scand. J. For. Res. 11, 261–268. doi:10.1080/02827589609382935
881 Buma, B., 2015. Disturbance interactions: characterization, prediction, and the potential for
882 cascading effects. Ecosphere 6, art70. doi:10.1890/ES15-00058.1
883 Cajander, A.K., 1949. Metsätyypit ja niiden merkitys. (Forest types and their importance).
884 (No. 56), Acta Forestalia Fennica. Suomen metsätieteellinen seura.
885 Eriksson, M., Neuvonen, S., Roininen, H., 2007. Retention of wind-felled trees and the risk
886 of consequential tree mortality by the European spruce bark beetle Ips typographus in
887 Finland. Scand. J. For. Res. 22, 516–523. doi:10.1080/02827580701800466
888 Eriksson, M., Pouttu, A., Roininen, H., 2005. The influence of windthrow area and timber
889 characteristics on colonization of wind-felled spruces by Ips typographus (L.). For. Ecol.
890 Manage. 216, 105–116. doi:10.1016/j.foreco.2005.05.044
891 Faccoli, M., 2002. Winter mortality in sub-corticolous populations of Ips typographus
892 (Coleoptera, Scolytidae) and its parasitoids in the south-eastern Alps. J. Pest Sci. (2004).
893 75, 62–68. doi:10.1034/j.1399-5448.2002.02017.x
894 Fahse, L., Heurich, M., 2011. Simulation and analysis of outbreaks of bark beetle infestations
895 and their management at the stand level. Ecol. Modell. 222, 1833–1846.
896 doi:10.1016/j.ecolmodel.2011.03.014
897 Frankel, S., 1998. User's guide to the Western Root Disease Model, version 3.0., Gen. Tech.
898 Rep. PSW-GTR-165. Albany, CA.

899 Franklin, A.J., Grégoire, J.-C., 1999. Flight behaviour of Ips typographus L. (Col.,
900 Scolytidae) in an environment without pheromones. Ann. For. Sci. 56, 591–598.
901 doi:10.1051/forest:19990706
902 Garbelotto, M., Gonthier, P., 2013. Biology, epidemiology, and control of Heterobasidion
903 species worldwide. Annu. Rev. Phytopathol. 51, 39–59. doi:10.1146/annurev-phyto-
904 082712-102225
905 Gardiner, B., Peltola, H., Kellomäki, S., 2000. Comparison of two models for predicting the
906 critical wind speeds required to damage coniferous trees. Ecol. Modell. 129, 1–23.
907 doi:10.1016/S0304-3800(00)00220-9
908 Giordano, L., Lione, G., Nicolotti, G., Gonthier, P., 2012. Effect of Heterobasidion annosum
909 s.l. root and butt rots on the stability of Norway spruce: an uprooting test, in: Capretti,
910 P., Comparini, P., Garbelotto, M., La Porta, N., Santini, A. (Eds.), Proceeding of the
911 XIII International Conference on Root and Butt Root of Forest Trees. Firenze (FI) – S.
912 Martino Di Castrozza (TN), Italy, 4th – 10th September 2012. University Press, Firenze,
913 pp. 247–250.
914 Gonzalez, R., Grégoire, J.-C., Drumont, A., Windt, N., 1996. A sampling technique to
915 estimate within-tree populations of pre-emergent Ips typographus (Col., Scolytidae). J.
916 Appl. Entomol. 120, 569–576. doi:10.1111/j.1439-0418.1996.tb01654.x
917 Grimm, V., Berger, U., Bastiansen, F., Eliassen, S., Ginot, V., Giske, J., Goss-Custard, J.,
918 Grand, T., Heinz, S.K., Huse, G., Huth, A., Jepsen, J.U., Jørgensen, C., Mooij, W.M.,
919 Müller, B., Pe'er, G., Piou, C., Railsback, S.F., Robbins, A.M., Robbins, M.M.,
920 Rossmanith, E., Rüger, N., Strand, E., Souissi, S., Stillman, R.A., Vabø, R., Visser, U.,
921 DeAngelis, D.L., 2006. A standard protocol for describing individual-based and agent-
922 based models. Ecol. Modell. 198, 115–126. doi:10.1016/J.ECOLMODEL.2006.04.023
923 Grimm, V., Berger, U., DeAngelis, D.L., Polhill, J.G., Giske, J., Railsback, S.F., 2010. The

924 ODD protocol: A review and first update. Ecol. Modell. 221, 2760–2768.
925 doi:10.1016/J.ECOLMODEL.2010.08.019
926 Grimm, V., Railsback, S.F., 2012. Pattern-oriented modelling: a “multi-scope” for predictive
927 systems ecology. Philos. Trans. R. Soc. Lond. B. Biol. Sci. 367, 298–310.
928 doi:10.1098/rstb.2011.0180
929 Grodzki, W., Gąsienica Fronek, W., 2017. Reproduction abilities of Ips typographus (L.)
930 (Coleoptera: Curculionidae, Scolytinae) in the stands damaged by the wind in 2013 in
931 the KoÊcieliska Valley (Tatra National Park). Folia For. Pol. 59, 258–264.
932 doi:10.1515/ffp-2017-0027
933 Grünwald, M., 1986. Ecological segregation of bark beetles (Coleoptera, Scolytidae) of
934 spruce. J. Appl. Entomol. 101, 176–187. doi:10.1111/j.1439-0418.1986.tb00846.x
935 Honkaniemi, J., Lehtonen, M., Väisänen, H., Peltola, H., 2017a. Effects of wood decay by
936 Heterobasidion annosum on vulnerability of Norway spruce stands to wind damage: a
937 mechanistic modelling approach. Can. J. For. Res. 47, 777–787. doi:10.1139/cjfr-2016-
938 0505
939 Honkaniemi, J., Ojansuu, R., Piri, T., Kasanen, R., Lehtonen, M., Salminen, H., Kalliokoski,
940 T., Mäkinen, H., 2014. Hmodel, a Heterobasidion annosum model for even-aged
941 Norway spruce stands. Can. J. For. Res. 44, 796–809. doi:10.1139/cjfr-2014-0011
942 Honkaniemi, J., Piri, T., Lehtonen, M., Siipilehto, J., Heikkinen, J., Ojansuu, R., 2017b.
943 Modelling the mechanisms behind the key epidemiological processes of the conifer
944 pathogen Heterobasidion annosum. Fungal Ecol. 25, 29–40.
945 doi:10.1016/j.funeco.2016.10.007
946 Hynynen, J., Salminen, H., Ahtikoski, A., Huuskonen, S., Ojansuu, R., Siipilehto, J.,
947 Lehtonen, M., Rummukainen, A., Kojola, S., Eerikäinen, K., 2014. Scenario analysis for
948 the biomass supply potential and the future development of Finnish forest resources (No.

949 302), Working papers of the Finnish Forest Research Institute.
950 Kautz, M., Schopf, R., Imron, M.A., 2014. Individual traits as drivers of spatial dispersal and
951 infestation patterns in a host–bark beetle system. Ecol. Modell. 273, 264–276.
952 doi:10.1016/j.ecolmodel.2013.11.022
953 Kautz, M., Schopf, R., Ohser, J., 2013. The "sun-effect": microclimatic alterations predispose
954 forest edges to bark beetle infestations. Eur. J. For. Res. 132, 453–465.
955 doi:10.1007/s10342-013-0685-2
956 Komonen, A., Schroeder, L.M., Weslien, J., 2011. Ips typographus population development
957 after a severe storm in a nature reserve in southern Sweden. J. Appl. Entomol. 135, 132–
958 141. doi:10.1111/j.1439-0418.2010.01520.x
959 Laasasenaho, J., 1982. Taper curve and volume functions for pine, spruce and birch (No.
960 108), Communicationes Instituti Forestalis Fenniae. Finnish Forest Research Institute.
961 Louis, M., Dohet, L., Grégoire, J.-C., 2016a. Fallen trees' last stand against bark beetles. For.
962 Ecol. Manage. 359, 44–50. doi:10.1016/j.foreco.2015.09.046
963 Louis, M., Grégoire, J.-C., Pélisson, P.-F., 2014. Exploiting fugitive resources: How long-
964 lived is "fugitive"? Fallen trees are a long-lasting reward for Ips typographus
965 (Coleoptera, Curculionidae, Scolytinae). For. Ecol. Manage. 331, 129–134.
966 doi:10.1016/j.foreco.2014.08.009
967 Louis, M., Toffin, E., Gregoire, J.-C., Deneubourg, J.-L., 2016b. Modelling collective
968 foraging in endemic bark beetle populations. Ecol. Modell. 337, 188–199.
969 doi:10.1016/j.ecolmodel.2016.07.008
970 Långström, B., Lindelöw, Å., Schroeder, M., Björklund, N., Öhrn, P., 2009. The spruce bark
971 beetle outbreak in Sweden following the January-storms in 2005 and 2007.
972 Mulock, P., Christiansen, E., 1986. The threshold of successful attack by Ips typographus on
973 Picea abies: A field experiment. For. Ecol. Manage. 14, 125–132. doi:10.1016/0378-

974 1127(86)90097-6
975 Müller, M.M., Sievänen, R., Beuker, E., Meesenburg, H., Kuuskeri, J., Hamberg, L.,
976 Korhonen, K., 2014. Predicting the activity of Heterobasidion parviporum on Norway
977 spruce in warming climate from its respiration rate at different temperatures. For. Pathol.
978 44, 325–336. doi:10.1111/efp.12104
979 Möykkynen, T., Kontiokari, J., 2001. Spore deposition of Heterobasidion annosum coll. in
980 Picea abies stands of North Karelia, eastern Finland. For. Pathol. 31, 107–114.
981 doi:10.1046/j.1439-0329.2001.00229.x
982 Nêmec, V., Zumr, V., Starý, P., 1993. Studies on the nutritional state and the response to
983 aggregation pheromones in the bark beetle, Ips typographus (L.) (Col., Scolytidae). J.
984 Appl. Entomol. 116, 358–363. doi:10.1111/j.1439-0418.1993.tb01208.x
985 Neuvonen, S., Nevalainen, S., Silver, T., Viiri, H., 2017. Kirjanpainajan feromoniseurannan
986 tulokset 2016 (No. 50), Metsätuhot vuonna 2016, Luonnonvara- ja biotalouden tutkimus.
987 Neuvonen, S., Tikkanen, O.-P., Viiri, H., 2016. Neljä vuotta kansallista
988 kirjanpainajaseurantaa: feromoniseurannan tulokset 2015 ja muita havaintoja, in:
989 Nevalainen, S., Pouttu, A. (Eds.), Metsätuhot Vuonna 2015. p. 36.
990 Oliva, J., Julio Camarero, J., Stenlid, J., 2012. Understanding the role of sapwood loss and
991 reaction zone formation on radial growth of Norway spruce (Picea abies) trees decayed
992 by Heterobasidion annosum s.l. For. Ecol. Manage. 274, 201–209.
993 doi:10.1016/j.foreco.2012.02.026
994 Oliva, J., Samils, N., Johansson, U., Bendz-Hellgren, M., Stenlid, J., 2008. Urea treatment
995 reduced Heterobasidion annosum sl root rot in Picea abies after 15 years. For. Ecol.
996 Manage. 255, 2876–2882. doi:10.1016/j.foreco.2008.01.063
997 Oliva, J., Thor, M., Stenlid, J., 2010. Reaction zone and periodic increment decrease in Picea
998 abies trees infected by Heterobasidion annosum s.l. For. Ecol. Manage. 260, 692–698.

doi:10.1016/j.foreco.2010.05.024

Peltola, H., Ikonen, V.-P., Gregow, H., Strandman, H., Kilpeläinen, A., Venäläinen, A., Kellomäki, S., 2010. Impacts of climate change on timber production and regional risks of wind-induced damage to forests in Finland. For. Ecol. Manage. 260, 833–845. doi:10.1016/j.foreco.2010.06.001

Peltola, H., Kellomäki, S., Väisänen, H., Ikonen, V.-P., 1999. A mechanistic model for assessing the risk of wind and snow damage to single trees and stands of Scots pine, Norway spruce, and birch. Can. J. For. Res. 29, 647–661. doi:10.1139/cjfr-29-6-647

Peltola, H.M., 2006. Mechanical stability of trees under static loads. Am. J. Bot. 93, 1501–11. doi:10.3732/ajb.93.10.1501

Peltonen, M., 1999. Bark beetles at forest edges: Effects on species occurrence. Julkaisuja/Reports 26. University of Helsinki.

Piri, T., 2003. Early development of root rot in young Norway spruce planted on sites infected by Heterobasidion in southern Finland. Can. J. For. Res. 33, 604–611. doi:10.1139/x02-200

Piri, T., Valkonen, S., 2013. Incidence and spread of Heterobasidion root rot in uneven-aged Norway spruce stands. Can. J. For. Res. 43, 872–877. doi:10.1139/cjfr-2013-0052

Poolak, L., 1975. Overwinter of spruce bark beetles (Ips spp.). Metsanduslikud Urimused 12, 315–325.

Potterf, M., Bone, C., 2017. Simulating bark beetle population dynamics in response to windthrow events. Ecol. Complex. 32, 21–30. doi:10.1016/J.ECOCOM.2017.08.003

Pukkala, T., Möykkynen, T., Thor, M., Rönnberg, J., Stenlid, J., 2005. Modeling infection and spread of Heterobasidion annosum in even-aged Fennoscandian conifer stands. Can. J. For. Res. 35, 74–84. doi:10.1139/x04-150

R Development Core Team, 2015. R: A language and environment for statistical computing

3.1.3.

Raffa, K.F., Berryman, A.A., 1983. Physiological aspects of lodgepole pine wound responses to a symbiont of the mountain pine beetle, Dendroctonus ponderosae (Coleoptera:Scolytidae). Can. Entomol. 115, 723–734. doi:10.4039/Ent115723-7

Raffa, K.F., Grégoire, J.-C., Staffan Lindgren, B., 2015. Natural History and Ecology of Bark Beetles, in: Vega, F.E., Hofstetter, R.W. (Eds.), Bark Beetles. pp. 1–40. doi:10.1016/B978-0-12-417156-5.00001-0

Safranyik, L., Wilson, B., 2006. The mountain pine beetle : a synthesis of biology, management, and impacts on Lodgepole Pine. Natural Resources Canada, Canadian Forest Service, Pacific Forestry Centre, Victoria, British Columbia.

Salminen, H., Lehtonen, M., Hynynen, J., 2005. Reusing legacy FORTRAN in the MOTTI growth and yield simulator. Comput. Electron. Agric. 49, 103–113. doi:10.1016/j.compag.2005.02.005

Schlyter, F., Anderbrant, O., 1993. Competition and Niche Separation between Two Bark Beetles: Existence and Mechanisms. Oikos 68, 437–447. doi:10.2307/3544911

Schlyter, F., Birgersson, G., Leufvén, A., 1989. Inhibition of attraction to aggregation pheromone by verbenone and ipsenol. J. Chem. Ecol. 15, 2263–2277. doi:10.1007/BF01014114

Seidl, R., Baier, P., Rammer, W., Schopf, A., Lexer, M.J., 2007. Modelling tree mortality by bark beetle infestation in Norway spruce forests. Ecol. Modell. 206, 383–399. doi:10.1016/j.ecolmodel.2007.04.002

Seidl, R., Müller, J., Hothorn, T., Bässler, C., Heurich, M., Kautz, M., 2016. Small beetle, large-scale drivers: how regional and landscape factors affect outbreaks of the European spruce bark beetle. J. Appl. Ecol. 53, 530–540. doi:10.1111/1365-2664.12540

Seidl, R., Schelhaas, M.-J., Lexer, M.J., 2011. Unraveling the drivers of intensifying forest

1049 disturbance regimes in Europe. Glob. Chang. Biol. 17, 2842–2852. doi:10.1111/j.1365-
1050 2486.2011.02452.x
1051 Seidl, R., Schelhaas, M.-J., Rammer, W., Verkerk, P.J., 2014. Increasing forest disturbances
1052 in Europe and their impact on carbon storage. Nat. Clim. Chang. 4, 806–810.
1053 doi:10.1038/nclimate2318
1054 Stenlid, J., Redfern, D.B., 1998. Spread within tree and stand, in: Woodward, S., Stenlid, J.,
1055 Karjalainen, R., Hütterman, A. (Eds.), Heterobasidion Annosum: Biology, Ecology,
1056 Impact and Control2. Wallingford, UK: CAB International, pp. 125–141.
1057 Wermelinger, B., 2004. Ecology and management of the spruce bark beetle Ips
1058 typographus—a review of recent research. For. Ecol. Manage. 202, 67–82.
1059 doi:10.1016/j.foreco.2004.07.018
1060 Weslien, J., Annila, E., Bakke, A., Bejer, B., Eidmann, H., Narvestad, K., Nikula, A., Ravn,
1061 H.P., 1989. Estimating risks for spruce bark beetle (Ips typographus (L.)) damage using
1062 pheromone-baited traps and trees. Scand. J. For. Res. 4, 87–98.
1063 doi:10.1080/02827588909382549
1064 Weslien, J., Regnander, J., 1990. Colonization densities and offspring production in the bark
1065 beetle Ips typographus (L.) in standing spruce trees. J. Appl. Entomol. 109, 358–366.
1066 doi:10.1111/j.1439-0418.1990.tb00064.x
1067 Whitney, R.D., Fleming, R.L., Zhou, K., Mossa, D.S., 2002. Relationship of root rot to black
1068 spruce windfall and mortality following strip clear-cutting. Can. J. For. Res. 32, 283–
1069 294. doi:10.1139/X01-194
1070 Witzell, J., Berglund, M., Rönnberg, J., 2011. Does temperature regime govern the
1071 establishment of Heterobasidion annosum in Scandinavia? Int. J. Biometeorol. 55, 275–
1072 284. doi:10.1007/s00484-010-0333-1
1073 Woodward, S., Stenlid, J., Karjalainen, R., Hütterman, A., 1998. Heterobasidion annosum:

1074 Biology, Ecology, Impact and Control. Wallingford, UK: CAB International.
1075 Vuokila, Y., Väliaho, H., 1980. Viljeltyjen havumetsiköiden kasvatusmallit = Growth and
1076 yield models for conifer cultures in Finland (No. 99), Metsäntutkimuslaitoksen
1077 julkaisuja. Metsäntutkimuslaitos.
1078 Äijälä, O., Koistinen, A., Sved, J., Vanhatalo, K., Väisänen, P., 2014. Hyvän metsänhoidon
1079 suositukset – Metsänhoito (Recommendations for good forest management – forest
1080 management) [in Finnish]. Forestry Development Centre Tapio.
1081

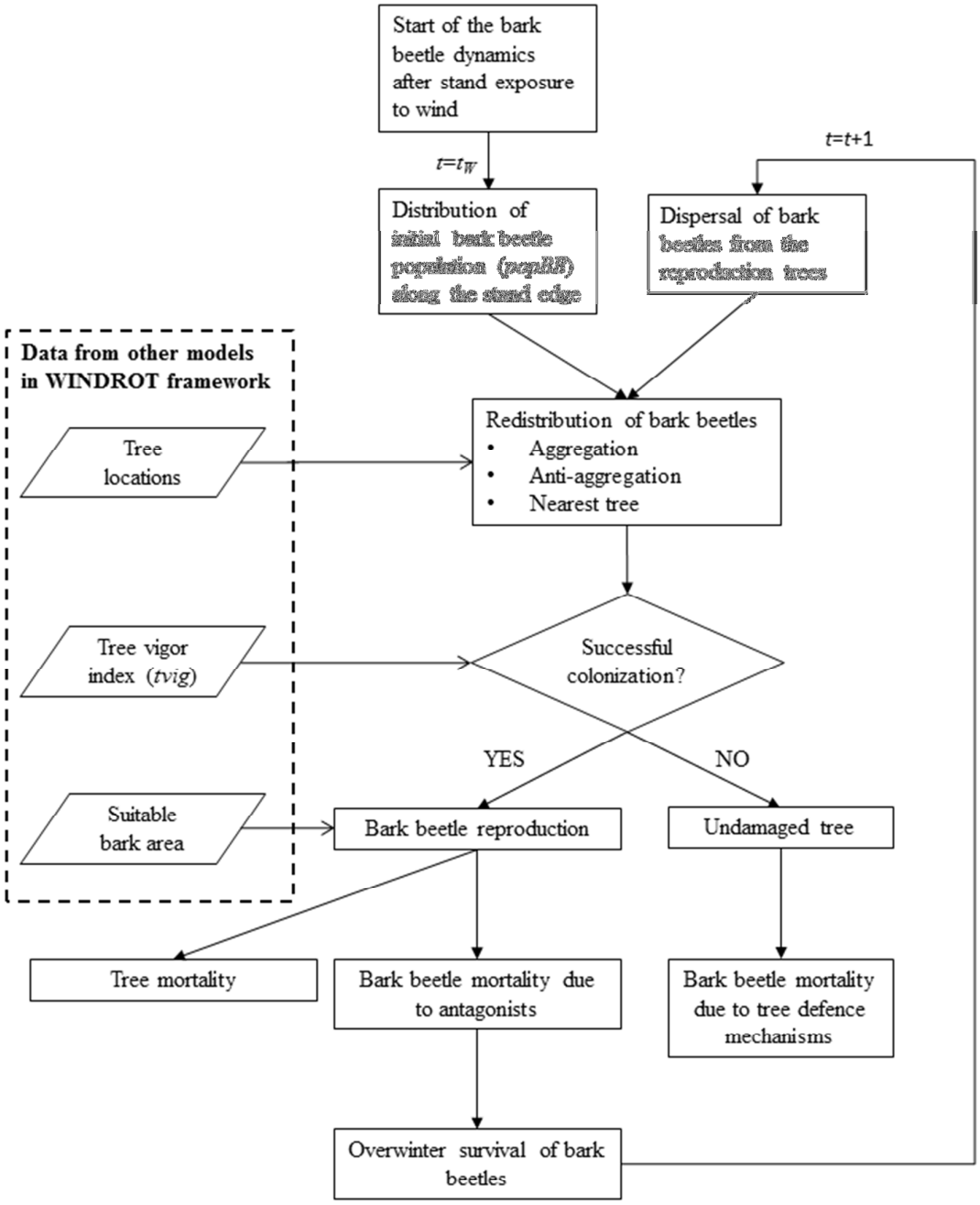

1082

1083 Figure 1.

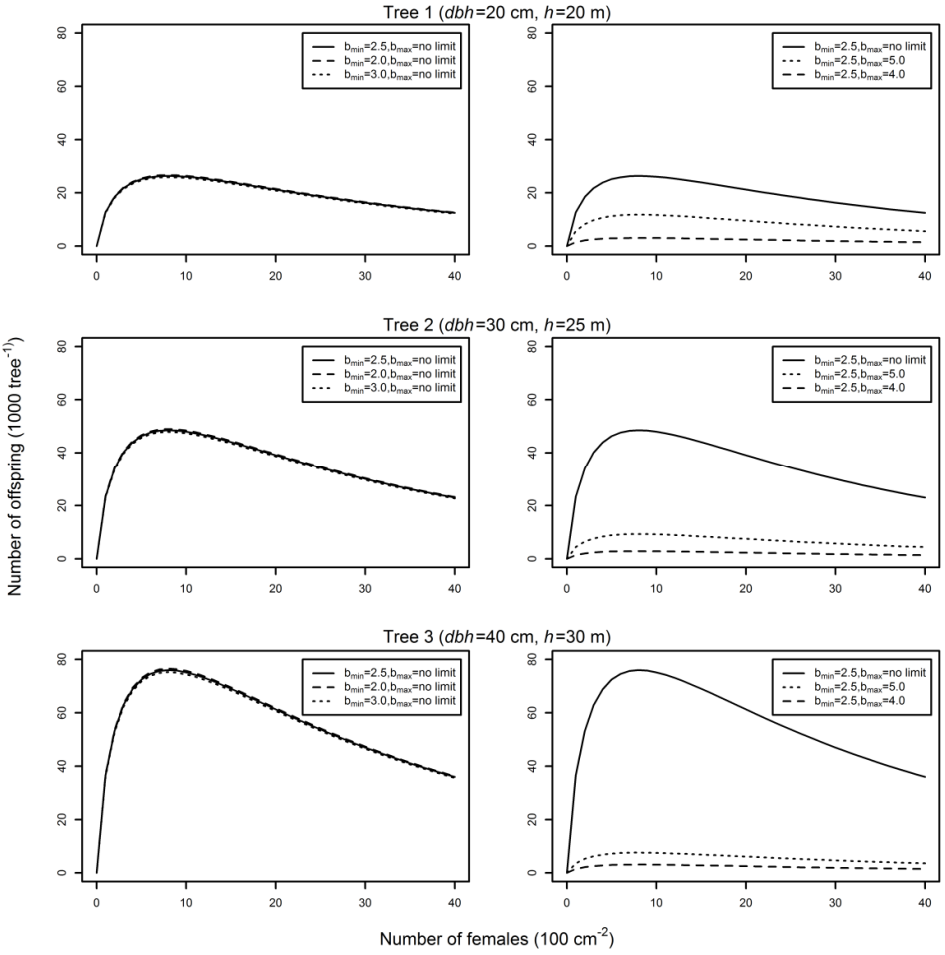

1084

1085 Figure 2.

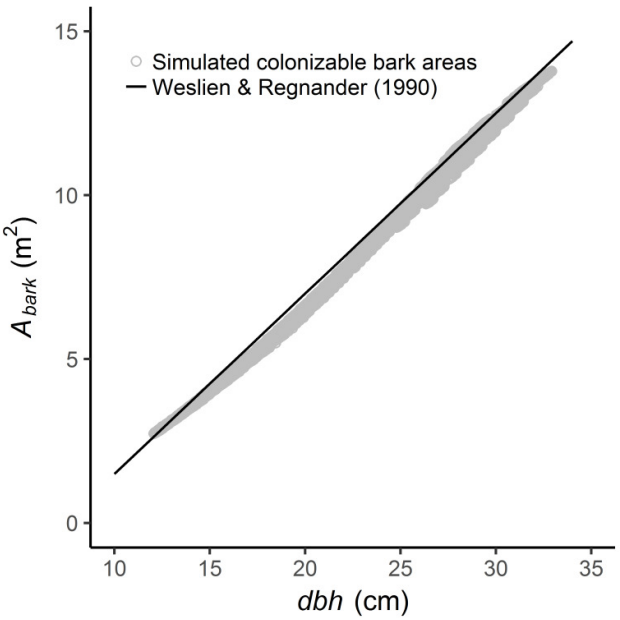

1086

1087 Figure 3.

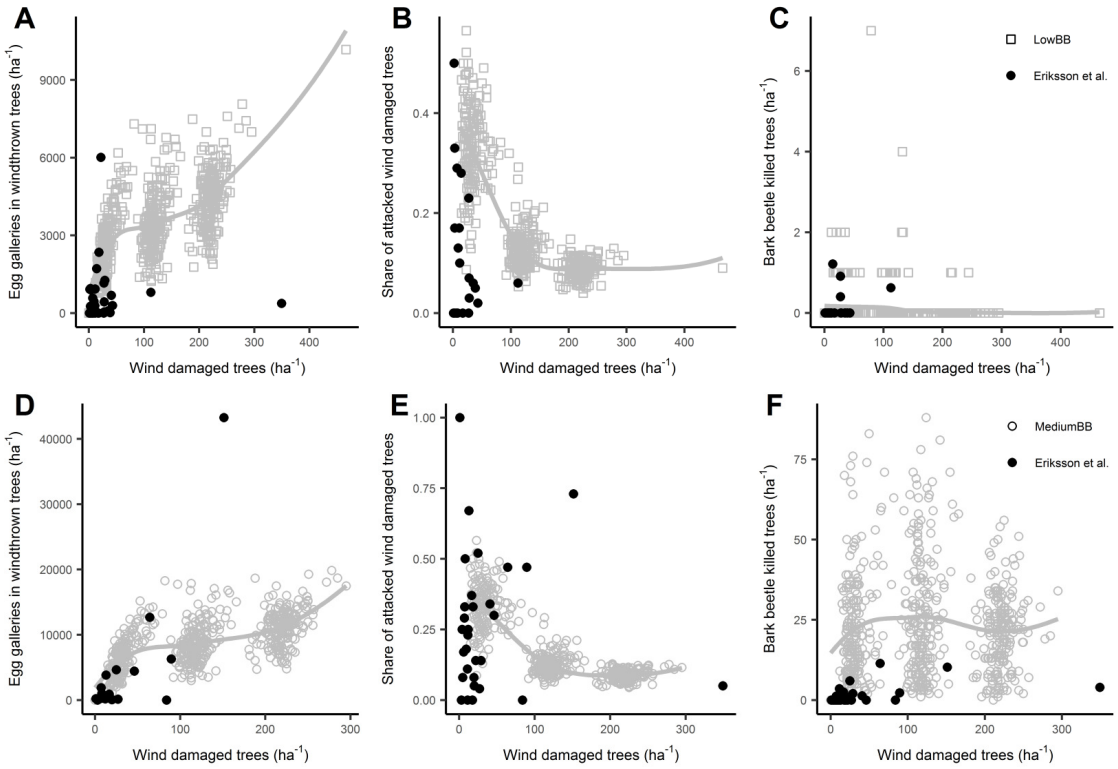

1088

1089 Figure 4.

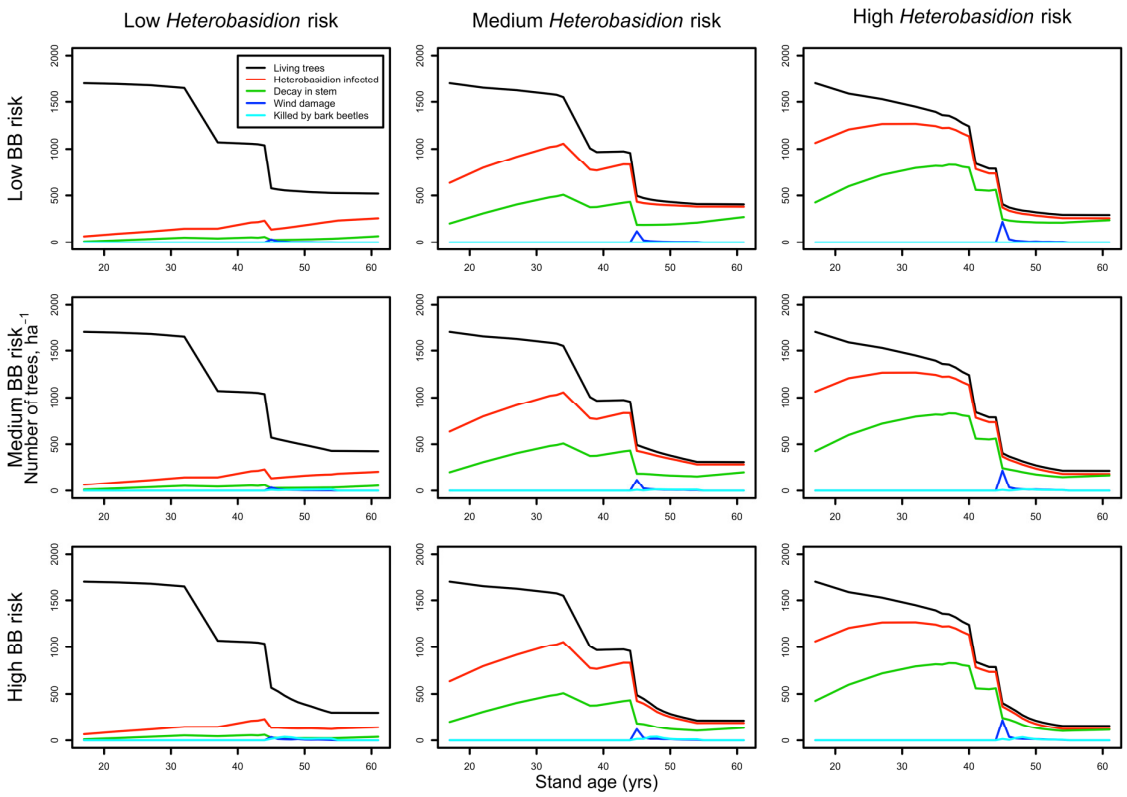

1090

1091 Figure 5.

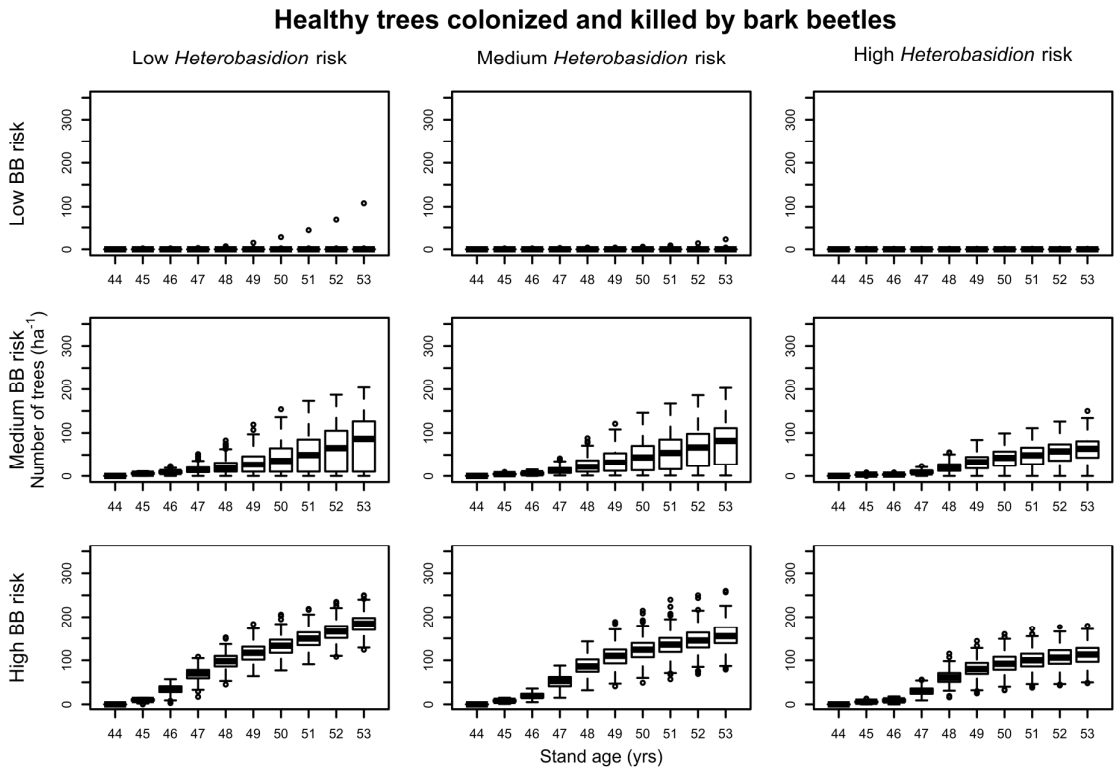

1092

1093 Figure 6.

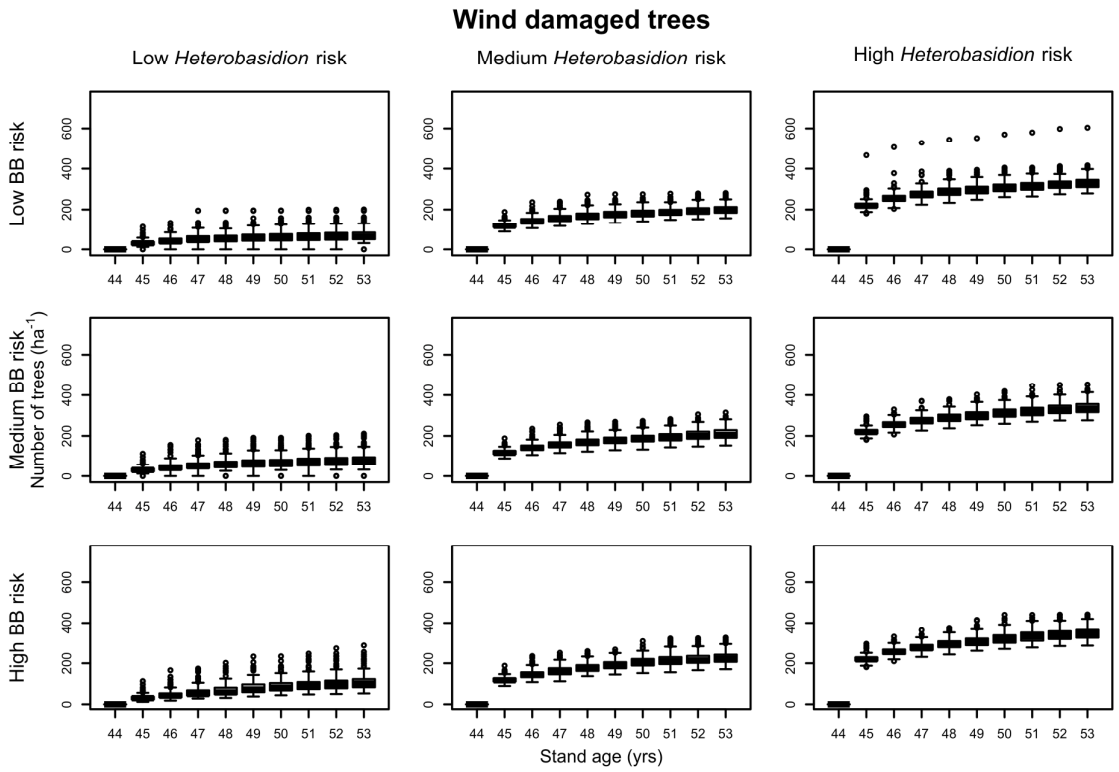

1094

1095 Figure 7.

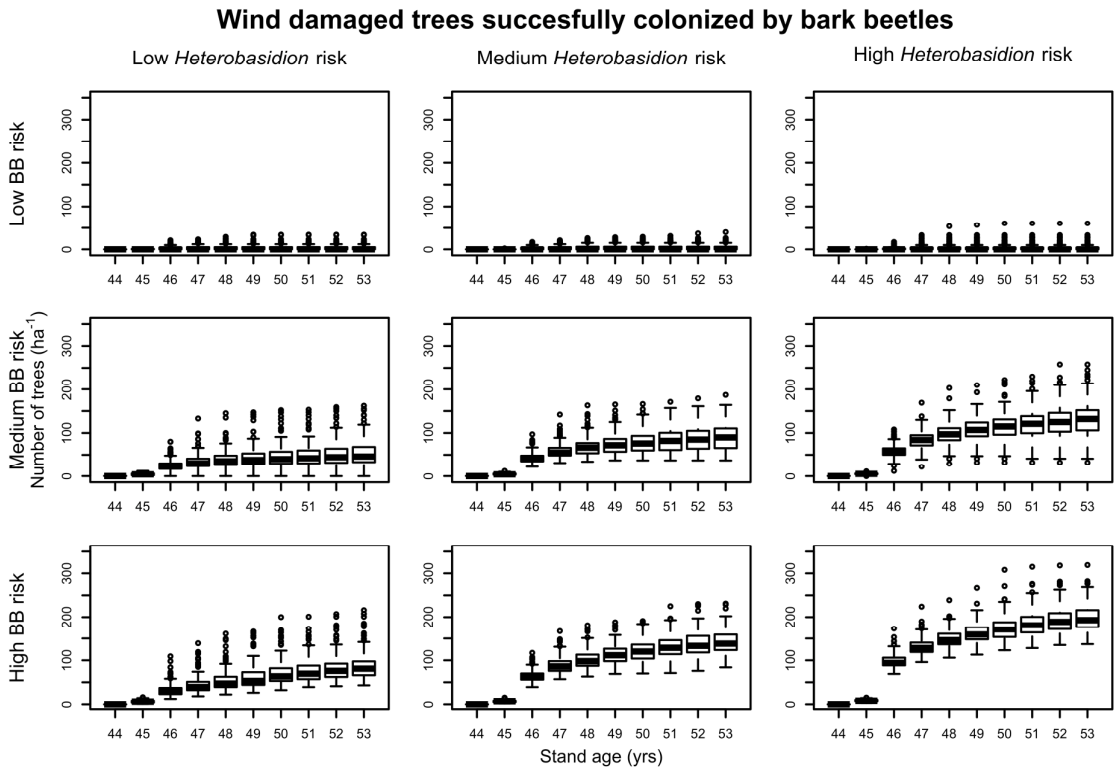

1096

1097 Figure 8.

Fig. 1. Conceptual diagram of BBDYN model structure during one simulation step (*i.e.* default of one year) and the linkage with data from other models of the WINDROT framework. (two columns wide)

Fig. 2. Sensitivity of the number of bark beetle offspring from a single tree to minimum (b_{min}) and maximum bark thickness (b_{max}) in three different trees. Left column graphs represent changes in b_{min} with constant b_{max} and right column graphs represent changes in b_{max} with constant b_{min}. (!1.5 columns wide!)

Fig. 3. The colonizable bark areas of infested trees from our simulations as a function of tree diameter at breast heigh. The line represents the model by Weslien and Regnander (1990) based on field data. (!one column wide!)

Fig 4. Comparison of stand level simulation output against field data by Eriksson et al. (2005, 2007). Figures on same rows are for same initial states: Figures A-C include low BB risk scenario output and data from Eriksson et al. with no previous bark beetle mortality in area and figures D-F include medium BB risk scenario output and data from Eriksson et al. with previous bark beetle mortality in area. Every figure in columns present same comparison of output: relation between the number of first year wind damaged trees and (A and D) total number of egg galleries in them; (B and E) share of attacked wind damaged trees out of all wind damaged trees; and (C and F) total number of trees killed by bark beetles during 4 years after the main wind disturbance event. (!two columns wide!)

Fig. 5. Number of living trees, number of *Heterobasidion* infected trees, number of trees with decay in stem, number of trees disturbed by wind (broken or fallen) and number of trees

killed by bark beetles. (!1.5columns wide!, colours for the e-version, B&W version provided for print)

Fig. 6. The cumulative number of trees killed by bark beetles over the 10-year simulation period in the 200 replications in nine different bark beetle – root rot scenarios. In the boxplots, median value is the line within the box and the box represents 25^{th} and 75^{th} percentiles. Whisker length is 1.5*box length and values beyond that are presented with open dots. (!1.5columns wide!)

Fig. 7. The cumulative number of wind damaged trees over the 10-year simulation period in the 200 replications in nine different bark beetle – root rot scenarios. Note the different scale on y-axis compared to the Fig. 6 & 8. In the boxplots, median value is the line within the box and the box represents 25^{th} and 75^{th} percentiles. Whisker length is 1.5*box length and values beyond that are presented with open dots. (!1.5columns wide!)

Fig. 8. The cumulative number of wind damaged trees successfully colonized by bark beetles over the 10-year simulation period in the 200 replications in nine different bark beetle – root rot scenarios. In the boxplots, median value is the line within the box and the box represents 25^{th} and 75^{th} percentiles. Whisker length is 1.5*box length and values beyond that are presented with open dots. (!1.5columns wide)

1144

Abbreviation	Explanation	Value	Unit	Source
User defined input variables				
t_W	Starting time of the wind damage and bark beetle simulations		years	
pop_{BB}	Initial bark beetle population		ha^{-1}	
Model parameters				
Dispersal				
D	Diffusion coefficient	644, 286 and 72 (strong, average and weak, respectively)	m^2 $season^{-1}$	Transformed from Fahse and Heurich (2011)
t_D	Time of dispersal	1	season	
r_{agg}	Aggregation catchment area radius	13.5	m	Transformed from Fahse and Heurich (2011)
R_{antagg}	Anti-aggregation catchment area radius	4.5	m	Transformed from Fahse and Heurich (2011)
Reproduction				
B_{min}	Minimum bark thickness	2.5	mm	Grünwald (1986)

	for bark beetles			
B_{max}	Maximum bark thickness for bark beetles	-	mm	Grünwald (1986)
Mortality of bark beetles				
$p_{find}(1)$	Probability for the trees to be found by antagonists when all trees in the vicinity ($dist<r_{pfind}$) are infested or dead due to bark beetles (< 1 year)	0.999		Fahse and Heurich (2011)
$p_{find}(0)$	As above, but when no infested trees or dead trees in the vicinity	0.03		Fahse and Heurich (2011)
r_{pfind}	Effective radius for the antagonists	28.2	m	Transformed from Fahse and Heurich (2011)
$p_{survival}$	Survival probability for bark beetles in a tree found by antagonists	0.05		Fahse and Heurich (2011)

Model variables

Colonization

N_{def}	Tree resistance threshold	$tree^{-1}$
tvig	Tree vigor index	*%*
BAi	Basal area of the latest	cm^2

	annual growth		
SA	Sapwood area		cm^2
i_{dbh}	Annual growth at *dbh*		cm
dbh	Tree diameter at breast height		cm
Reproduction			
D_{fl}	Density of offspring		100 cm^{-2}
D_{male}	Density of males in tree		100 cm^{-2}
D_{fem}	Density of females in tree	$2*D_{male}$	100 cm^{-2}
N_{male}	Number of males per tree		$tree^{-1}$
N_{fem}	Number of females per tree		$tree^{-1}$
N_{fl}	Number of offspring		$tree^{-1}$
A_{bark}	Colonizable bark area		100 cm^2
B	Bark thickness		mm
x	Relative tree height		
h	Tree height		m
l	Height within tree		m
l_{Bmin}	Height at B_{min}		m
l_{Bmax}	Height at B_{max}		m
h_{Abark}	Colonizable bark area length		m

Table 1. Model parameters and variables, their abbreviations and explanations as well as literature sources for parameter value.

1147

Parameter	Value	Std. error
a_1	19.98	0.84
a_2	0.19	0.01
a_3	-40.70	5.47
a_4	13.17	10.04
a_5	41.37	9.85
a_6	-54.48	6.04
a_7	26.91	1.61
u_j	0.88 mm	
ε_{lj}	1.08 mm	
φ	0.99	

1148 **Table 2.** Parameter values for the bark taper curve.

1149

1150

Parameter or submodel to be calibrated	Pattern used	Field data source	Scale	Major observations
Minimum and maximum bark thickness for bark beetles (b_{min} and b_{max})	Sensitivity to parameter changes		Tree	Model sensitive to maximum bark thickness (Fig. 2)
Reproduction	Colonizable bark area	Weslien and Regnander (1990)	Tree	Colonizable bark area with b_{min}=2.5 mm matches the field data (Fig. 3)
Reproduction	Number of egg galleries	Eriksson et al. (2005,2007)	Stand	Number of egg galleries slightly overestimated, but could be due to initial population (Fig. 4A, 4D)
Colonization and mortality of trees	Capability to attack wind damaged trees	Eriksson et al. (2005,2007)	Stand	Wind damaged trees colonized with similar rate as in field data (Fig. 4B, 4E)
Colonization and mortality of trees	Norway spruce mortality during 4 years after major wind event	Eriksson et al. (2005,2007)	Stand	Low risk scenario predicts well the spruce mortality, but medium risk scenario overestimates (Fig. 4C, 4F)
Initial bark beetle population level (input value, pop_{BB})	Outbreak capability/spruce mortality	Weslien et al (1989)	Stand	Spruce mortality due to bark beetles occurs only above the threshold of 15 000 beetles per trap as suggested by field data (Fig. 6)

Table 3. Model evaluation following the principles of pattern-oriented modelling and listing the used patterns as well as the data sources and the operational scale

1153

Variable	Value		
	Low	*Medium*	*High*
Number of previous generation stumps (N_{stump}, ha^{-1})	590	590	590
Spore density (D_{spore}, m^{-2} hr^{-1})	200	400	750
Number of infected previous generation stumps ($N_{infstump}$, ha^{-1})	0	118 (20 %)	295 (50 %)
Mean diameter of previous generation stumps ($d_{prestump}$, cm)	37	37	37
Share of *Heterobasidion parviporum* infections on previous generation stumps (P_{Hp})	0.9	0.9	0.9
Minimum distance between planted trees ($dist_{min}$, m)	1.0	1.0	1.0

1154 **Table 3.** Hmodel inputs with different root rot risk scenarios.

1155

APPENDIX 1.

1 General description of the models in WINDROT framework

1.1 MOTTI

The stand-level decision support system MOTTI (Hynynen et al., 2015, 2014; Salminen et al., 2005) is responsible for the host tree and stand dynamics in the WINDROT simulation framework. MOTTI simulates tree growth and stand dynamics in even-aged stands taking into account forest management operations during the rotation as well as the environmental conditions such as temperature sum, elevation or distance to sea. Climate is not included in the model. MOTTI divides the stand dynamics into two stages; young and old stand. First, the young stand dynamics from regeneration to dominant height of 8m are simulated with stand-level variables. Tree height and diameter are based on distribution models providing a link to the individual-tree-level models applied for the old stand (Siipilehto et al., 2014). The old stand models are spatially implicit simulating the stand development based on sample trees each representing a certain number of trees within one hectare (Hynynen et al., 2014).

The main assumption in WINDROT simulation framework is that every simulation starts from bare ground after a clearcut of a previous tree generation. Simulations are run for a one full rotation length defined by the user. MOTTI inputs include stand characteristics such as location, soil and site type as well as description of forest management operations. These forest management regime options include the intensity, number and timing of thinnings as well as the rotation length. In addition, potential soil preparation prior to regeneration can be defined as well as the type of regeneration (natural vs planting).

1.2 Hmodel

Hmodel (Honkaniemi et al., 2017b, 2014) is a mechanistic model with stochastic features to simulate the dynamics of root and butt rot causing fungal agent *Heterobasidion* species. Creating the spatial layout for WINDROT framework is part of Hmodel as MOTTI is spatially implicit. Hmodel consists of several submodels each responsible for one significant part of the fungal dynamics (e.g. spore infection, secondary spread). The primary infection process is a function of stump surface area, the spore density landing on the stump surface and the survival probabilities of heterokaryotic mycelia (two homokaryotic spores paired together forming a heterokaryotic structure) in stumps. If the mycelia survive and colonize a stump, the secondary spread will occur through the root system (roots simulated as a circle until root diameter of 2mm). Probability matrix and the overlap area between root systems of two trees or tree and stump are used to determine whether the fungus can infect a new host. If a secondary infection occurs, the mycelia will grow towards the stem base of the newly infected host tree with a given growth rate.

The fungus enters the host tree stem base at the border of heartwood and sapwood. Once the fungus enters the stem base, it starts to decay the wood into all directions. However, the tree defence mechanisms decrease the fungal growth rates, which are also dependent on the tracheid size (ie. growth is mediated by the number of cell walls that need to be degraded). Decay will progress upwards in the stem right after it enters the stem base, but will proceed to other parts of the root system only after 50% of the heartwood area in the stem base is decayed. Growth losses due to the disease are a function of the ratio between decayed sapwood area and healthy sapwood area. Disease causes mortality if the decay cover the whole cross-sectional area at stem base or if the decay area covered the cross-sectional area in 85% of the main roots at the root collar. Fungal survival in the degrading stump roots and roots of dead trees is a function of the diminishing amount of acid hydrolysable components (e.g. cellulose, hemicellulose and lignin).

The root rot also affects the tree mechanical stability against wind in two ways (Honkaniemi et al., 2017a). First, the decay column within the stem (decay height and width at the stem base based on the decay progress at time *t*) decreases the modulus of rupture of the stem. The decayed part is considered to offer no supportive strength and therefore the stem is considered as a hollow cylinder with only the outer rim of healthy wood offering mechanical stability for the tree. Second effect of root rot is in the root system, where the tree roots decrease their mechanical stability due to decay. The decay is assumed to proceed from the cross-sectional root centre outwards and if the cross-sectional area of healthy root at root diameter rd is less than the minimum cross sectional area offering mechanical strength against wind in a healthy tree, the root is considered to fail at that *rd* and reduce therefore the root-soil plate weight and diameter. This further decreases the tree stability against uprooting.

1.3 HWIND

HWIND (Peltola et al., 1999) is a mechanistic model to simulate wind disturbance effects on trees. It calculates the effect of static wind load on trees outputting critical wind speeds for each tree of the stand. HWIND predicts the critical wind speeds (given at a height of 10m at the edge of an upwind gap) for uprooting and stem breakage based on tree dimensions and stand characteristics. The tree dimensions include tree height and diameter at breast height as well as rooting depth, root-soil plate weight and modulus of rupture for tree species. HWIND can also include the effect of snow loading and combine that with wind disturbance. Critical wind speeds can be compared against local wind data and used to predict the wind disturbance.

2 Spatial layout of WINDROT framework

Disturbance dynamics are highly dependent on the stand spatial structure. Especially *Heterobasidion* dynamics depend on the tree locations due to the short distance secondary spread. As mentioned above, MOTTI is spatially implicit and therefore Hmodel was designed to include a module for setting up a spatially explicit stand structure (Honkaniemi et al., 2017b, 2014). In this module, the tree and stump locations are created randomly with a minimum distances specified for young trees, adult trees as well as for previous generation stumps. All of them are located within the 1 hectare (100m x 100m rectangle) stand (Fig. A1). Stand is surrounded by a buffer zone of 8 m with similar stand characteristics and forest management.

At the time of the wind exposure (t_W), a neighboring stand is cut from one of the bordering sides of the simulated area forming an upwind gap (Fig. A1). This gap is assumed to be a length of 10 times the height of the tallest tree in the stand as required by HWIND (Peltola et al., 1999).

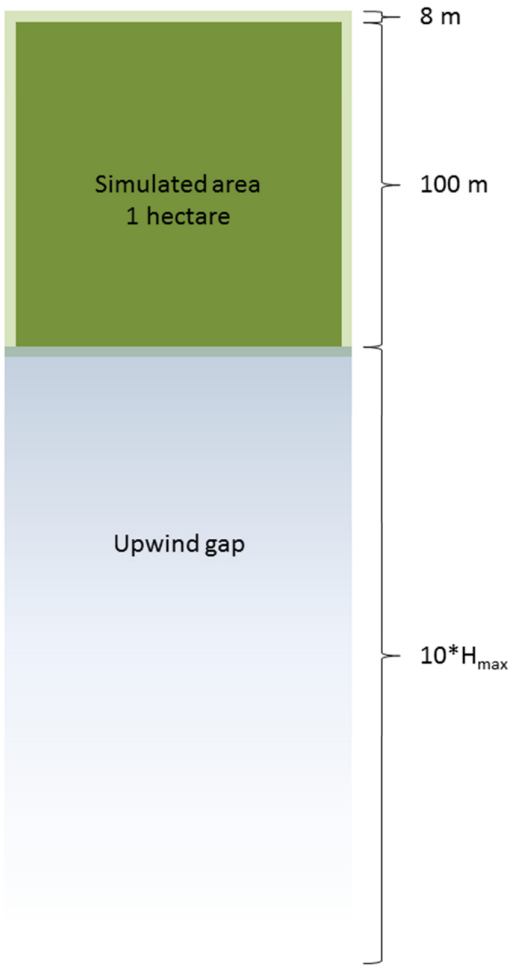

Fig. A1. Spatial layout of the simulation. Simulated area is a size of 1 hectare with a buffer zone of 8 m around it. This buffer zone is similar to the simulated stand and treated with same forest management regime with the exception of one bordering side which at the time of wind exposure t_W is cut down along with the neighboring stand forming a large upwind gap required by HWIND.

3 Stem form and wind damages

Wind damaged trees in our simulations tended to be slender as they are more prone to wind effects (see also Honkaniemi et al. 2017a). The *height/dbh* ratio of all the simulated trees was higher especially for wind fallen trees compared to healthy trees. This affected the colonizable bark area and further the number of attacking beetles as the threshold for emitting anti-aggregation pheromones was also lower. Even though healthy trees are attacked later in the simulation period and could thus be larger than the wind damaged trees falling or breaking mostly during the first years of the simulation, the similar pattern can be seen from the Fig. A2 with trees of only one year.

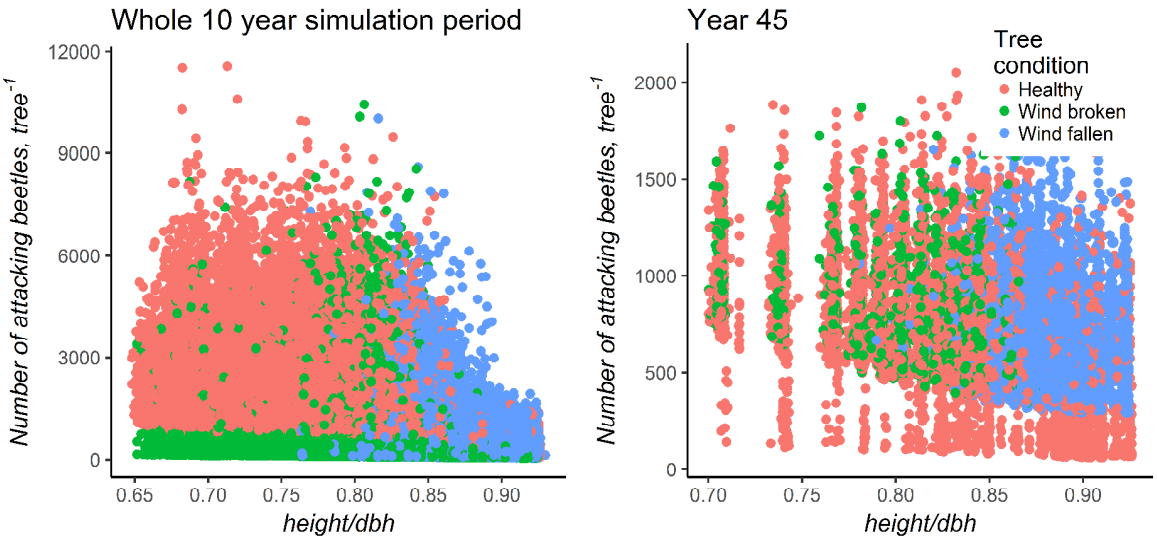

Fig. A2. Height/dbh ratio of all simulated trees under bark beetle attack against the number of attacking beetles in them during the whole simulation period or during one year. Trees are further classified by their wind damage status.

References:

1284 Honkaniemi, J., Lehtonen, M., Väisänen, H., Peltola, H., 2017a. Effects of wood decay by
1285 heterobasidion annosum on the vulnerability of Norway spruce stands to wind damage: A
1286 mechanistic modelling approach. Can. J. For. Res. 47. doi:10.1139/cjfr-2016-0505

1287 Honkaniemi, J., Ojansuu, R., Piri, T., Kasanen, R., Lehtonen, M., Salminen, H., Kalliokoski, T.,
1288 Mäkinen, H., 2014. Hmodel, a Heterobasidion annosum model for even-aged Norway spruce
1289 stands. Can. J. For. Res. 44, 796–809. doi:10.1139/cjfr-2014-0011

1290 Honkaniemi, J., Piri, T., Lehtonen, M., Siipilehto, J., Heikkinen, J., Ojansuu, R., 2017b.
1291 Modelling the mechanisms behind the key epidemiological processes of the conifer
1292 pathogen Heterobasidion annosum. Fungal Ecol. 25. doi:10.1016/j.funeco.2016.10.007

1293 Hynynen, J., Salminen, H., Ahtikoski, A., Huuskonen, S., Ojansuu, R., Siipilehto, J., Lehtonen,
1294 M., Eerikäinen, K., 2015. Long-term impacts of forest management on biomass supply and
1295 forest resource development: a scenario analysis for Finland. Eur. J. For. Res. 134, 415–431.
1296 doi:10.1007/s10342-014-0860-0

1297 Hynynen, J., Salminen, H., Ahtikoski, A., Huuskonen, S., Ojansuu, R., Siipilehto, J., Lehtonen,
1298 M., Rummukainen, A., Kojola, S., Eerikäinen, K., 2014. Scenario analysis for the biomass
1299 supply potential and the future development of Finnish forest resources (No. 302), Working
1300 papers of the Finnish Forest Research Institute.

1301 Peltola, H., Kellomäki, S., Väisänen, H., Ikonen, V.-P., 1999. A mechanistic model for
1302 assessing the risk of wind and snow damage to single trees and stands of Scots pine, Norway
1303 spruce, and birch. Can. J. For. Res. 29, 647–661. doi:10.1139/cjfr-29-6-647

1304 Salminen, H., Lehtonen, M., Hynynen, J., 2005. Reusing legacy FORTRAN in the MOTTI
1305 growth and yield simulator. Comput. Electron. Agric. 49, 103–113.
1306 doi:10.1016/j.compag.2005.02.005

1307 Siipilehto, J., Ojansuu, R., Miina, J., Hynynen, J., Valkonen, S., Saksa, T., 2014.
1308 Metsikönvarhaiskehityksen kuvaus MOTTI-ohjelmistossa [In Finnish]. (No. 286), Metlan
1309 Työraportti/ Metla Working Paper.